CHALMERS

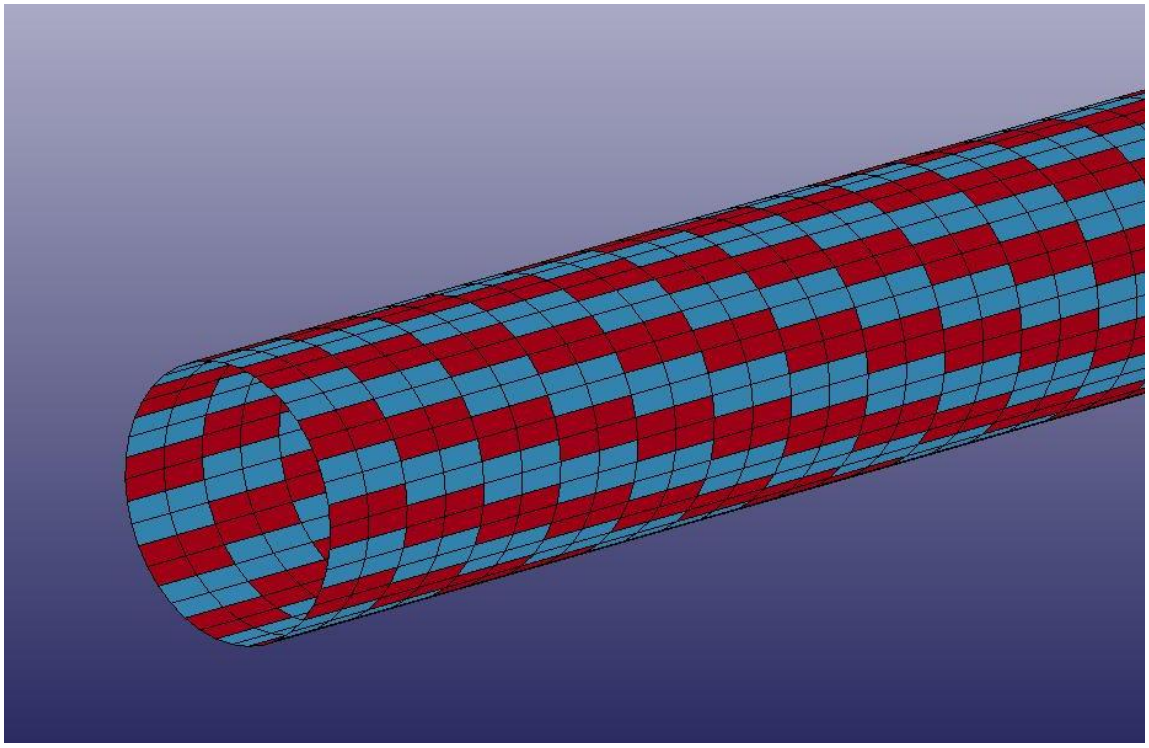

Transient FE-modelling of wood cells exposed to steam explosion

Strain rate effects and deformation mechanism

Master of Science Thesis in the Master's Programme Structural Engineering and Building Technology

BJÖRN ALWERUD

Department of Civil and Environmental Engineering
Division of Structural Engineering
Concrete Structures
CHALMERS UNIVERSITY OF TECHNOLOGY
Göteborg, Sweden 2013

Master's Thesis 2013:30

MASTER'S THESIS 2013:30

Transient FE-modelling of wood cells exposed to steam explosion

Strain rate effects and deformation mechanism

Master of Science Thesis in the Master's Programme Structural Engineering and Building Technology

BJÖRN ALWERUD

Department of Civil and Environmental Engineering
Division of Structural Engineering
Concrete Structures
CHALMERS UNIVERSITY OF TECHNOLOGY
Göteborg, Sweden 2013

Transient FE-modelling of wood cells exposed to steam explosion
Master of Science Thesis in the Master's Programme Structural Engineering and Building Technology
BJÖRN ALWERUD

Examensarbete / Institutionen för bygg- och miljöteknik,
Chalmers tekniska högskola 2013:30

Department of Civil and Environmental Engineering
Division of Structural Engineering
Concrete Structures
Chalmers University of Technology
SE-412 96 Göteborg
Sweden
Telephone: + 46 (0)31-772 1000

Cover: Simple model of a wood cell in LS-DYNA

Chalmers Reproservice / Department of Civil and Environmental Engineering
Göteborg, Sweden 2013

Transient FE-modelling of wood cells exposed to steam explosion
Strain rate effects and deformation mechanism
Master of Science Thesis in the Master's Programme Structural Engineering and Building Technology
BJÖRN ALWERUD
Department of Civil and Environmental Engineering
Division of Structural Engineering
Concrete Structures
Chalmers University of Technology

ABSTRACT

Steam explosion is a method for decomposing and opening up the cell structure of wood and other biomass in order to make it more available for production of e.g. biofuels. In order to optimise this process, the finite element method could be a valuable tool. Due to the explosive nature of the process, high strain rates of the material could be expected, meaning that static finite element models might not be sufficient in capturing the real response of the material. Therefore, the purpose of this work was to investigate how a transient finite element model could be set-up in order to simulate the process.

A literature study was made to find an appropriate geometric and constitutive representation of spruce wood at the level of a single cell. It was found that while some data regarding these parameters is available in literature, some information is lacking regarding the mechanical properties of the cell wall constituents. In particular, no data describing the strain rate dependence of the wood polymers was found in literature. It was however concluded that the matrix polymers, i.e. lignin and hemicellulose, are likely to be strain rate dependent due to their amorphous molecular structure. Using the knowledge gained from the literature study, a simple model of a single spruce wood cell subjected to steam explosion was created and simulations were performed in LS-DYNA.

In the result, a torsional deformation mechanism was observed due to a reorientation of the reinforcing cellulose fibrils in the direction of the load. Although the simple model did not include strain rate dependence of the material, it was observed that the strain rates given by the simulations were high. This indicates that introducing a strain rate dependence to the constitutive relation might significantly influence the results. However, it has not been possible to derive material properties of strain rate dependence and it is suggested to derive these from experiments on other amorphous polymers such as plastics, or from tests performed on wood in the macro-scale. The project also derived ideas on how the representation, i.e. geometry, materials, load and boundary conditions can be improved.

Key words: Wood cell, strain rate, transient finite element modelling, steam explosion, mechanism

Transient finita element-modellering av träceller utsatta för ångexplosion
Töjningshastighetseffekter och deformationsmekanism
Examensarbete inom Structural Engineering and Building Technology
BJÖRN ALWERUD
Institutionen för bygg- och miljöteknik
Avdelningen för Konstruktionsteknik
Betongbyggnad
Chalmers tekniska högskola

SAMMANFATTNING

Ångexplosion är en metod som används för att sönderdela och öppna upp cellstrukturen hos trä och annan biomassa i syfte att göra materian mer tillgänglig för produktion av t.ex. biobränslen. För att optimera denna process kan finita element-metoden vara ett användbart verktyg. På grund av det explosiva förloppet i processen kan höga töjningshastigheter av materialet förväntas, vilket innebär att statiska finita element-modeller inte lyckas fånga det verkliga beteendet hos materialet. Syftet med detta arbete var därför att undersöka hur en transient finita element-modell kan utformas för att simulera processen. En litteraturstudie genomfördes för att finna en lämplig geometrisk och konstitutiv representation av barrträ på nivån av en enskild cell. Det kunde konstateras att viss data finns tillgänglig i litteraturen, medan annan information, så som de mekaniska egenskaperna hos beståndsdelarna i cellväggen, saknas. I synnerhet hittades inga data som beskriver töjningshastighetsberoende hos materialen. Det konstaterades dock att de två komponenterna hos matrismaterialet, d.v.s. lignin och hemicellulosa, sannolikt är töjningshastighetsberoende på grund av deras amorfa molekylstrukturer.

Informationen från litteraturstudien användes för att skapa en enkel modell av en enskild träcell utsatt för ångexplosion och simuleringar utfördes i LS-DYNA. Resultaten visade att cellen vrids när den deformeras. Vridning uppstår på grund av en omorganisering i spänningsriktningen av de förstärkande cellulosafibrillerna. Den enkla modellen inkluderade inte töjningshastighetsberoende hos materialet men det kunde konstateras att töjningshastigheterna i simuleringarna var höga, vilket tyder på att införandet av ett töjningshastighetsberoende till det konstitutiva sambandet troligen skulle påverka resultaten påtagligt. Det har emellertid inte varit möjligt att härleda sådana materialegenskaper för de enskilda träpolymererna. Det föreslås istället att dessa data härleds från experiment på andra amorfa polymerer såsom plaster, eller från tester på trä i makroskala. Projektet presenterar också idéer om hur representationen av geometri, material, last och randvillkor hos den enkla modellen kan förbättras.

Nyckelord: Träcell, töjningshastighet, transient finita element modellering, ångexplosion, mekanism

Contents

Preface

This master's thesis project has been carried out at Chalmers University of Technology during the period April 2012 to June 2013. The project started on the initiative of my supervisor Rasmus Rempling after he came in contact with the department for chemical and biological engineering at Chalmers for assistance in modelling wood in steam explosion. The subject is not a typical topic for structural engineers, and the project has been rather interdisciplinary. It has been challenging but also very interesting to work in this way and it is my belief that a lot can be gained from considering a problem from different viewpoints and to share knowledge between different fields of research.

I would like to thank Rasmus Rempling for his enthusiastic support and guidance through the project, as well as the nice people at the division of structural engineering at Chalmers. I would also like to thank Marik and my family for their great support and patience along the way.

Göteborg June 2013

Björn Alwerud

Explanation of expressions

Softwood	Wood coming from either spruce or pine
Wood cell	A softwood tracheid, i.e. a tube-like, microscopic element, many of which build up a piece of wood
Cell structure	Several wood cells as organised in a piece of wood
Cell wall	The solid part of a wood cell
Lumen	The hollow space inside wood cells
Middle lamella	A layer mainly of lignin, present between two cell walls in the cell structure of wood, serving to cement the cells together
Latewood	The part of an annual ring that consists of cells with relatively thick walls and small diameter
Earlywood	The part of an annual ring that consists of cells with relatively thin walls and large diameter
Transition wood	The intermediate between latewood and earlywood
Microfibril	A nanoscopic element consisting of cellulose, hemicellulose and lignin
Cellulose fibril	The cellulose part of the microfibril. Consists of bundles of cellulose chains

Microfibril angle	The angle of the microfibril to the longitudinal axis of a wood cell
Cellulose fibril angle	The angle of the cellulose fibril to the longitudinal axis of a wood cell (equal to the microfibril angle)
Strain rate	Unit strain per unit time [s^{-1}]
Effective strain rate	Unit of effective strain per unit time [s^{-1}]
Crystalline polymer	Polymer in which the molecule chains are ordered in a specific pattern
Amorphous polymer	Polymer which is non-crystalline, i.e. the molecule chains have a disordered structure
Strain energy density	The product of strain and stress accumulated over time
Enzymatic hydrolysis	Conversion of carbohydrates into basic sugar molecules, e.g. cellulose into glucose, by the use of enzymes
Specific area	The total available area per unit weight of a material

1 Introduction

1.1 Background

In later years, the need for reducing the world consumption of fossil fuels has become increasingly important. Biofuels such as ethanol and biogas have been proposed as renewable alternatives to fossil fuels, but they have also been criticised for being produced by crops that could be potential food sources, or for using cropland that could be used for food production.

For this reason, forest products such as wood has become of increasing interest for the production of biofuels. The abundance of such biomass is considerable, forests covering about 31% of the world's land surface, see FAO (2005). The function of wood and other cellulosic materials as renewable energy sources is however limited by the need for refining processes in order to make the components more available for digestion and conversion into biofuels. These processes often require extensive use of chemicals and energy.

Steam explosion is a process in which wood chips are cooked with saturated steam, at high temperature and pressure, followed by rapid decompression. This causes a decomposition of the cell structure of the wood chips and produces a pulp. The process has for long been used for the production of paper and fibreboard, see Kokta and Ahmed (1998). In recent years, steam explosion has become of interest as a means of increasing the energy efficiency in biofuel production. The treatment increases the porosity and the specific area of the cell structure and thus makes the material more susceptible to enzymatic hydrolysis and subsequent conversion into biofuels.

In order to understand and optimise the steam explosion process, finite element modelling could be a valuable tool. A model can be used for studying the deformation mechanisms of the cell structure and parameters can be varied in order to optimise the process. Previous FE-modelling of wood, at the level of individual cells, has been aimed mainly at deriving properties of wood material in the macro-scale. Lately, modelling of the wood cell structure has also been performed with the purpose of increasing energy efficiency in mechanical pulping processes used for paper production, e.g. in De Magistris (2005).

Such pulping processes as well as steam explosion both involve high loading rates and consequently rapid straining of the material. The processes are of a dynamic character and strain rate effects are likely to play a role in the mechanical response of the material. The high strain rates might have an influence on the mechanical properties and deformation mechanisms, and static FE-models might be incapable of describing this behaviour. Therefore it would be desirable to establish a model to be used in transient finite element analysis.

1.2 Aim and purpose

The general purpose of this work was to examine if the determining internal mechanisms of wood cells exposed to steam explosion are strain rate dependent. Furthermore, it was investigated how the finite element software LS-DYNA could be used to model the cell wall at different strain rates.

The objective was to establish principles for modelling the behaviour of a single wood cell exposed to a rapidly increased internal pressure. The objective was divided into two parts where the first part consisted of a literature review on the subject. The following questions were to be answered:

- What is the structure to be modelled, i.e. the structure of a wood cell?
- What mechanical properties of the cell-wall should be used?
- How does the material respond to high strain rates?
- What are the characteristics of the load in steam explosion?
- Which are the possible determining internal mechanisms?
- How is wood modelled at the cell wall level?

The second part was to determine principles for modelling in LS-DYNA regarding the following aspects:

- Geometry
- Constitutive relation
- Boundary conditions
- Load

1.3 Scientific approach

Finite element modelling in mechanical and structural engineering is generally dealing with larger structures and well-known materials for which a substantial amount of experimental data is available. In this study, geometries were very small, ranging from a number of nm to a few mm. This offers challenges when using traditional concepts of mechanics since the behaviour of materials in the very small scale is hard to determine experimentally and since the properties of an isolated component can be very different from the properties of the same component when it is incorporated in a small structure. Chemical interactions between the different components play an important role, something that can be unfamiliar to mechanical and structural engineers. Hence, although timber might be a well-known material in engineering, the mechanical behaviour of its basic components is not so well understood.

Furthermore, wood presents a complex, multilevel hierarchical structure and no model can take into account the exact structure on every level. Instead, idealisations must be made and homogenisation can be used to simplify the heterogeneous structures. In steam explosion of wood, the raw material is generally wood chips which consist of a large number of wood cells. The individual wood cells in turn have anisotropic properties due to their heterogeneous ultrastructure. In this work, the choice was made to focus on how individual wood cells can be modelled and to study the particular mechanisms arising from their heterogeneous structure. The results of such a model can hopefully be used in further modelling at various levels.

The approach in the project was to gather knowledge about the real structure of wood at different levels, and of the different components that build up wood and, in the next step, make assumptions where necessary due to the lack of knowledge about mechanical properties and structure. Regarding material properties, there was a need for gathering information from different fields of research, such as chemical and mechanical engineering and assumptions can be based on properties of other materials that have been tested experimentally and that resemble the components of wood.

Also, wood is a biological material and the functions of the structure and materials are shaped to the needs of the living tree. Keeping this in mind gives a better understanding of the structure and mechanical properties of wood.

1.4 Limitations

The work considered only softwood and the modelling was limited to a single, isolated cell. The representation of load was limited to internal pressure and the complex interplay between flow porosity and pressure, arising in steam explosion, was beyond the scope of this work. No comparison was made between different wood species or different pulping processes. The modelling was made in LS-DYNA and no other software was used for comparison.

1.5 Method

In the first part of the objective, a literature review was made in order to achieve an understanding of the wood cell structure, material properties and of the steam explosion process. Focus of the review was initially put on the actual properties and structure of the material, rather than on how the structure could be modelled. Later in the process attention was turned to what had previously been done in the field of FE-modelling of wood.

In the second part of the objective a simple model was created using the knowledge gained from the literature review. The process of developing the model was to a certain extent about learning the software and the pre-processing tool available for LS-DYNA.

2 Literature review

In order to establish a finite element model of a wood cell exposed to steam explosion it is necessary to know the structure of the cell as well as the properties of the materials that build up the structure. It is also necessary to find an adequate representation of the load involved in steam explosion. In this chapter, the structure and mechanical properties of wood and its components is presented and discussed on basis of the current level of knowledge. The steam explosion process is then described followed by a discussion of the mechanical response of wood cells to the load involved in the process.

2.1 The hierarchical structure of wood

The information about the structure of wood presented in this chapter is achieved from Dinwoodie (2010) unless specific reference is given in the text. A characteristic feature of wood is its complex hierarchical structure. At each level of hierarchy the material can be considered as a heterogeneous composite. The material is a natural product which is shaped by the environment in which it has grown and the structure and properties vary between species and between individuals of the same species. In order to determine a representative model of a softwood cell, one must consider several factors including tree species, cell type and from what part of the tree the cell is taken. For that reason it is necessary to have a basic understanding of the material from the macro level to the ultrastructural level.

Macro level

By macro level is meant here a piece of softwood which is free from imperfections such as knots. At this level, wood is known as an anisotropic material with three main directions, defined in relation to the fibre direction of the wood: longitudinal (L), radial (R) and tangential (T), see Figure 1. Generally, the strength and stiffness of wood is greatest in the longitudinal direction, parallel to the fibres, and greater in the radial direction than in the tangential direction.

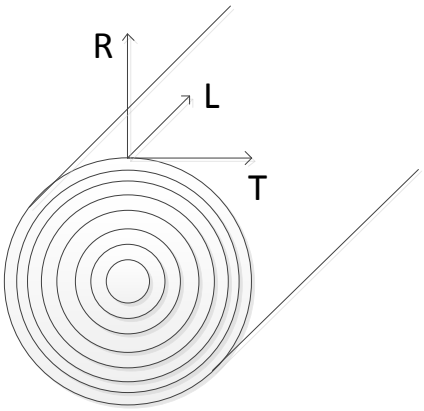

Figure 1 Cross-section of a tree log with its three main directions

Annual ring level

The macro level material consists of a number of annual rings. One annual ring represents the growth of a tree during one year. It can be divided into three layers with different densities: Earlywood, transitionwood and latewood. Earlywood is formed in the spring season and has relatively low density. The main function of earlywood cells is to transport water and nutrients which is why the cell walls are thin in relation to the

width of the cells. Latewood is formed in the fall at the end of the growth season and serves mainly to provide strength and stiffness to the tree trunk. The cell walls are thick in relation to cell width and the density is relatively high. The latewood appears as darker strands in the wood. Transition wood is the intermediate between earlywood and latewood. It is formed in the summer season and serves both for transportation and support.

Cell level

In the microscopic scale, wood consists of a network of cells oriented mainly in the longitudinal direction of the tree trunk, see Figure 2. The solid part of the cellular network consists of cell walls, held together by a lamella of lignin. The hollow part of each cell is called the lumen. In addition to the longitudinal cells, a smaller amount of cells, called "rays", are oriented in the radial direction. The lumens of adjacent cells are connected at certain points by so called "pits" i.e. circular holes in the cell wall which allow for flow of water and nutrients between cells.

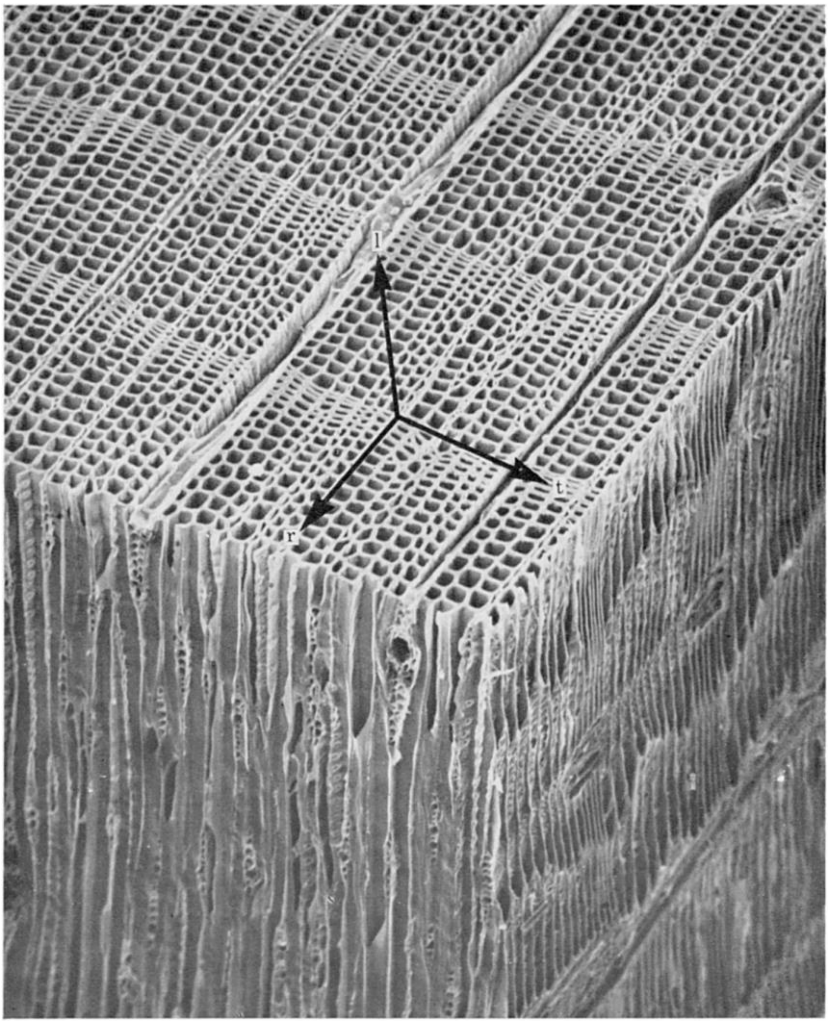

Figure 2 Microscopic view on a piece of softwood revealing the cell structure, from Barret (1981)

Softwood consists of two types of cells, parenchyma and tracheids. The tracheid is the dominating cell type, making up about 95% of the wood tissue. They are oriented in the longitudinal direction of wood and serve both for support and for conduction of water and nutrients up the tree. Tracheids can be considered as long and slender tubes,

with a length of 3-4 mm in mature wood. The width is about 30-40 µm for earlywood and 20-30 µm for latewood cells. Parenchyma cells are shorter and wider than tracheids and occur mainly as rays to conduct water and nutrients in the radial direction of the tree. In the following sections, the term "wood cell" or "fibre" will refer to a tracheid cell.

Ultrastructural level

The cell wall is commonly regarded as a layered structure consisting of a primary wall, P, and a secondary wall, S. The secondary wall is in turn divided into the three layers S1, S2 and S3, see Figure 3.

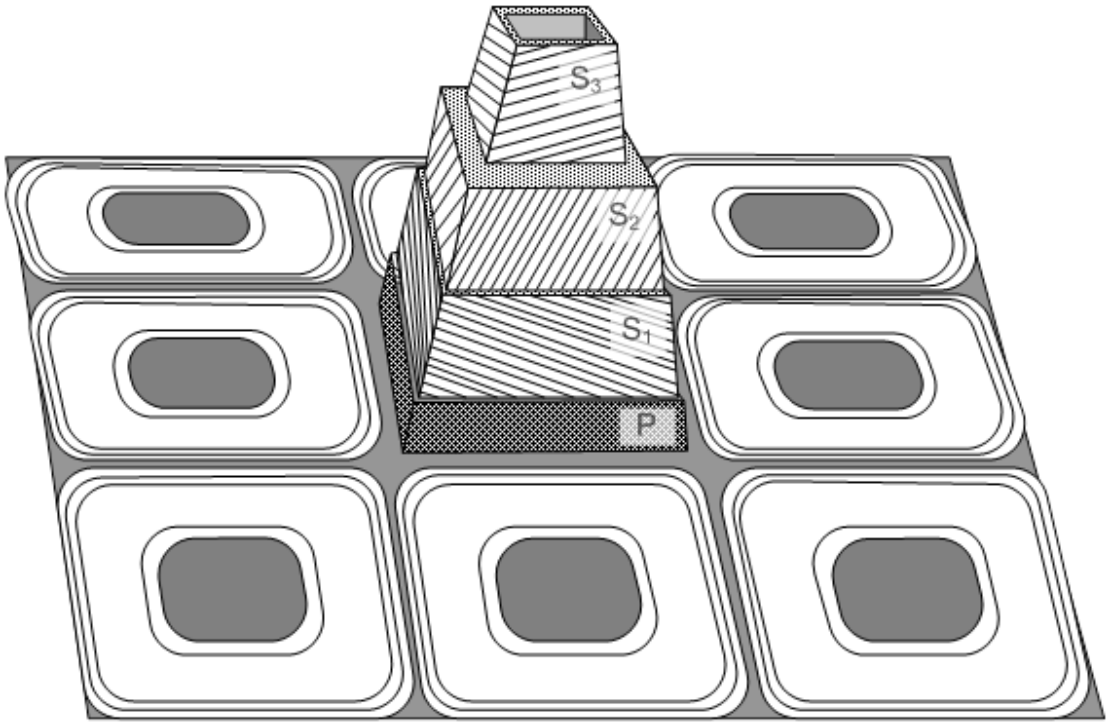

Figure 3 *Schematic view of the cell wall layers of a wood cell. The striped pattern represents the orientation of cellulose fibrils in each layer, from Hoffmeyer (1995).*

The layers of the cell wall differ in thickness, chemical composition and in the angle of cellulose fibrils to the longitudinal axis of the cell, see Table 1. The P-layer is thin and contains randomly oriented cellulose fibrils, making it a rather isotropic structure. The S1 and S3 layers are also thin and contain cellulose fibrils which are arranged in a helical pattern with an angle of about 50-90° to the longitudinal axis of the cell. The S2-layer is by far the thickest layer and it also has the greatest content of cellulose. Therefore, it is often considered as the structurally dominant layer of the cell wall. Also in S2, the cellulose fibrils are arranged in a helical pattern but the angle is much smaller than in S1 and S3. This means that stiffness and strength of S2 is much greater in the longitudinal direction than in the tangential and radial directions of the cell. The properties of the cell wall layers vary greatly depending on from where in the tree the cell comes from. For instance, the thickness of the S2-layer is considerably greater for latewood than for earlywood cells.

Table 1 *Properties of the various cell wall layers. The chemical fractions are in per cent by volume, Qing and Mishnaevsky (2009)*

Cell wall layer	Thickness [µm]	MFA [°]	Cellulose [%]	Hemicellulose [%]	Lignin [%]
M	0,25	-	0	62	38
P	0,1	random	12	26	62
S1	0,2 - 0,3	50 - 90	35	30	35
S2	1,4 - 4,0	0 - 45	50	27	23
S3	0,03 - 0,04	50 - 90	45	35	20

The cell wall ultimately consists of three components: cellulose, hemicellulose and lignin. Cellulose is a polymer chain of about 5000-10000 glucose molecules held together by strong covalent bonds, Mishnaevsky and Qing (2008). Several cellulose chains form fibrils which have a crystalline structure and high stiffness and strength. Amorphous, i.e. non-crystalline portions of cellulose also occurs periodically along the length of the cellulose fibrils. This amorphous cellulose has lower stiffness and strength than crystalline cellulose and is more sensitive to moisture. Hemicelluloses, is a group of carbohydrates which, compared to cellulose, have a more amorphous structure with a lower degree of polymerisation and crystallinity. This makes the material softer and weaker and also more sensitive to moisture than cellulose. Lignin also has an amorphous structure but is chemically different to cellulose and hemicellulose. It is an aromatic polymer consisting of phenyl groups and forms large, branched molecules.

The arrangement of cellulose, hemicelluloses and lignin, is often described as a fibre reinforced composite. In this model, cellulose fibrils are considered to act as reinforcement, embedded in a matrix of hemicellulose and lignin. The matrix material is however not a homogenous blend of hemicelluloses and lignin but has a rather ordered structure. The exact structure of the microfibril is not known but it is often modelled with a core of crystalline cellulose surrounded by a layer of hemicellulose and non-crystalline cellulose chains. The next layer is a coating of lignin which cements the microfibrils together to form the different layers of the cell wall. It also serves to protect the hydrophilic hemicelluloses and non-crystalline parts of cellulose from moisture, see Figure 4.

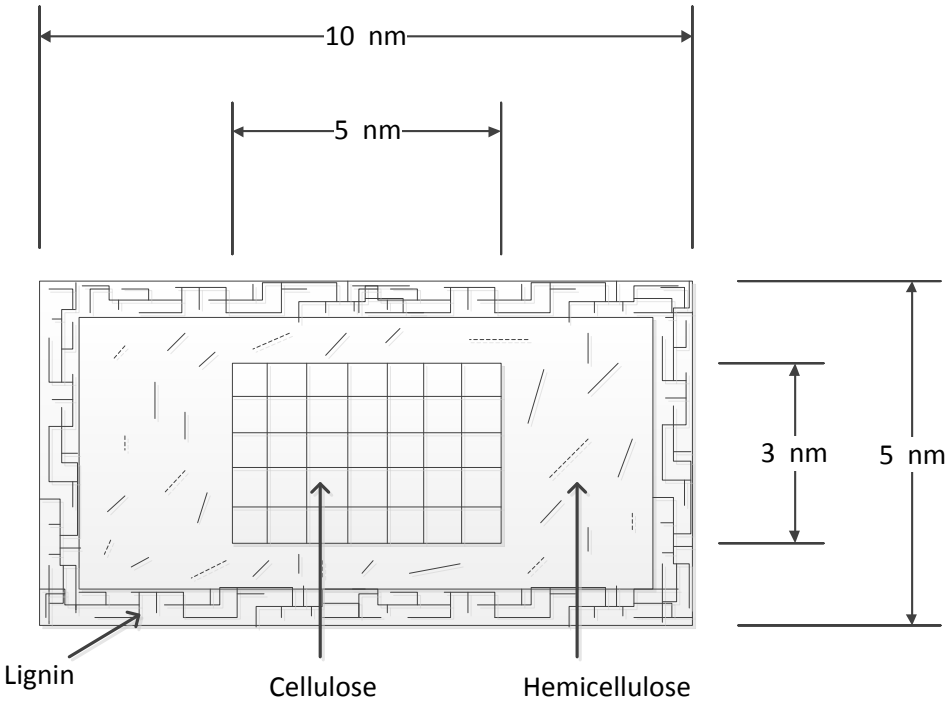

Figure 4 *Model of the cross-section of a microfibril with approximate dimensions*

2.2 Mechanical properties of the wood polymers

Mechanical properties of wood at macro level can be determined experimentally by performing tests on pieces of clear wood. Determining properties of the individual wood polymers cellulose, hemicellulose and lignin, by tensile or compressive testing, is more difficult. A problem that arises, when performing experiments on isolated cellulose, hemicellulose or lignin, is that the components show different behaviour when isolated than when incorporated in the structure, see Cousins (1978). Instead, properties of the individual components can be calculated by molecular modelling, or estimated on basis of the behaviour in the larger scale.

Density

Due to the porous cell structure of wood, the density of the material in the macro-scale is much smaller than the density of the cell wall. The density of the cell wall in a dry state has been measured to approximately 1500 kg/m^3, see Domone and Illstone (2010). Densities of the individual wood polymers are found in Table 2. Since moisture causes swelling of the cell wall, it will also influence its density.

Table 2 *Density values for the wood polymers, Thuvander, Kifetew and Berglund (2002)*

Wood polymer	**Density [kg/m^3]**
Cellulose	1550
Hemicellulose	1500
Lignin	1300

Elastic properties

The elastic properties of the cell wall polymers are highly influenced by temperature and moisture. For the amorphous wood polymers, i.e. hemicellulose, lignin and non-crystalline cellulose, a glass transition temperature,T_g, can be identified. Below T_g the material is in a relatively brittle, glassy state, and above T_g the material is in a more viscous, soft state. The glass transition temperature is influenced by moisture, which has a plasticising effect on the polymers, meaning that T_g decreases with increasing moisture content. This applies in particular for the carbohydrate amorphous polymers, i.e. hemicellulose and amorphous cellulose which adsorb water by hydrogen bonding. Lignin is less hydrophilic and therefore less influenced by moisture. According to Salmén (1982), when saturated with water, the hemicellulose and non-crystalline cellulose can be assumed to be in the soft state at room temperature while water saturated lignin is likely to be in the glassy state at temperatures up to 100°C. The crystalline cellulose does not soften in the same way as the amorphous polymers. However, the cellulose crystallites start to decompose at temperatures above 300°C, Kim et al. (2001). In the steam explosion process, water saturated wood chips are heated to temperatures around 200°C, see Section 2.3. These severe conditions imply that all the wood polymers, except the crystalline parts of the cellulose, are likely to be in a soft state before the pressure is released.

When determining elastic properties of the wood polymers, most effort has been dedicated to cellulose since it is considered the dominating constituent in the mechanical behaviour of the cell wall. For hemicellulose and lignin, data is much scarcer and contains greater uncertainties. Studies have shown that both the hemicellulose and lignin molecules have a preferred orientation in the cell wall along the microfibrils. This means that all the wood polymers are likely to have anisotropic mechanical properties. In Table 3, a set of elastic constants, recommended for modelling by Salmén (2004), are depicted. The index "x" corresponds to the property along the cellulose fibril and "y" corresponds to the property in the plane normal to the cellulose fibril axis, Salmén (2004).

Table 3 Elastic properties for model calculations of cellulose, hemicellulose and lignin, Salmén (2004)

	Dry conditions (12 % moisture, 20°C)	Wet conditions (20°C)
Cellulose (crystalline)		
E_x	134 GPa	134 GPa
E_y	27.2 GPa	27.2 GPa
G	4.4 GPa	4.4 GPa
ν	0.1	0.1
Hemicellulose		
E_x	2.0 GPa	0.02 GPa
E_y	0.8 GPa	0.008 GPa
G	1.0 GPa	0.01 GPa
ν	0.2	0.2
Lignin		
E_x	2.0 GPa	2.0 GPa
E_y	1.0 GPa	1.0 GPa
G	0.6 GPa	0.6 GPa
ν	0.3	0.3

The periodically occurring segments of amorphous cellulose in the cellulose fibrils have much lower stiffness and strength than the crystalline parts of cellulose. Chen et al. used molecular modelling to derive elastic properties of amorphous cellulose. A value of Young's modulus, $E = 10.42$ GPa and a Poisson's ratio of $\nu = 0.23$ was achieved and a transition temperature of about 220°C was also calculated, see Chen et al. (2004). According to Salmén (1982) it can be assumed that water penetrates into the amorphous cellulose when the material is immersed in water, and softens the material. If that is the case, the amorphous cellulose is likely to be softened at a significantly lower temperature than 220°C. Therefore, in the case of steam explosion the amorphous cellulose can be assumed to be in the soft state.

For both amorphous cellulose and lignin, data regarding elastic properties in the soft state was scarcely found in literature. However, for lignin in the soft state, Salmén

(1982) estimated the Young's modulus as $E = 0.06$ GPa and the shear modulus as $G = 0.0225$ GPa.

Yield stress and strength

Experimental values of yield stress and ultimate strength of the individual wood polymers were scarcely found in literature. A value of the yield stress in shear for the hemicellulose-lignin matrix of τ_y=11 MPa has been suggested by Keckes et al. (2003). This value was used in modelling by Saavedra Flores et al. (2011) who applied the Von Mises yield condition to achieve a value of σ_y=19 MPa. For the moist conditions and high temperature in steam explosion, the yield stress of the matrix is possibly even lower than this value.

On the level of an entire cell wall, some data of ultimate strength is available which might be used for estimating yielding and strength properties of the individual wood polymers. Tensile tests of individual spruce wood fibres were performed by Eder et al. (2008). The cells were tested under wet conditions, at normal temperature. Tensile strength values of around 550 MPa for early wood cells, and around 800 MPa for latewood cells were achieved. The values were calculated on basis of the respective cell wall cross-sectional areas. The lower strength of earlywood cells was explained by an earlier crack initiation due to tension buckling arising from the helical microfibril structure of the cell wall, Eder et al. (2008). This phenomenon is discussed further in Section 2.4.2

Influence of strain rate

Strain rate is a measure of how fast a material is strained, i.e. unit strain per unit time. Since strain has no dimension, the unit of strain rate is $1/s$, or s^{-1}. High strain rates are present where loading rates are high, such as in explosion and impact situations and it is known to have a great influence on the mechanical properties of many materials. For instance, in concrete, high strain rate leads to a changed fracture pattern and an increase in stiffness, strength and deformation capacity, see Leppänen (2004). In steam explosion of wood, the cell structure is exposed to a rapidly increased internal pressure (see Section 2.3) and high strain rates of the cell wall material can be expected. Therefore, it would be desirable to include strain rate dependence of the materials in a finite element model of a wood cell exposed to steam explosion. However, for the cell wall constituents, cellulose, hemicellulose and lignin, there appears to be a considerable lack of data regarding the influence of high strain rates. Instead, conclusions might be drawn on basis of experiments on wood at macro level, or from experiments on materials that are chemically similar to cellulose hemicellulose and lignin.

For wood at the macro-level, it has been shown that for very high loading rates, the behaviour is different than under static loading. Mindess and Madsen studied the fracture of wood under impact loading by a falling weight striking a simply supported, wooden beam at mid-span. They found that a tensile crack developed along a straighter path, from the bottom of the beam, than would be the case for a corresponding static load, see Mindess and Madsen (1986). Also tensile tests on wood have shown that both the fracture energy and the tensile strength increase with increasing loading rate, see Holmberg (1998). Uhmeier and Salmén studied the influence of temperature and strain rate on the radial compression behaviour of wet spruce. The stress strain curves shown in Figure 5 are characterised by an initially elastic region, followed by a plateau region at which the stress is approximately

constant and then by a radical increase in stress. The bold curves correspond to water saturated specimens while the thin curves correspond to specimens near the fibre saturation point, i.e. where the cell walls are completely wetted but where there is no "free" water present in the lumens of the cells. The tests showed that for both water contents, the plateau region started at a higher stress for the higher strain rate. The greater increase in stress for the fully saturated specimens in the plateau region was explained by the resistance coming from pressing out the lumen water at the high strain rate, Uhmeier and Salmén (1996).

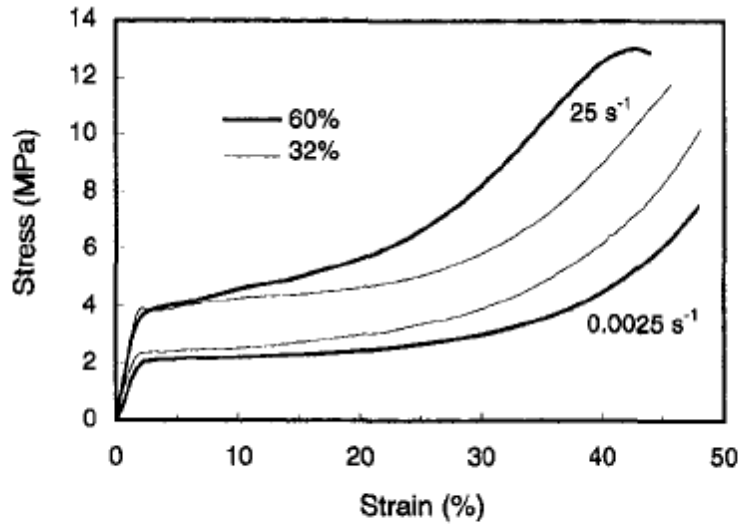

Figure 5 *Compression tests of wet spruce at a low and a high strain rate. The bold lines correspond to fully saturated specimens and the thin lines to specimens approximately at the fibre saturation point, Uhmeier and Salmén (1996).*

Also at the level of individual cells, time dependent behaviour has been observed. Tensile tests on individual wood fibres, performed by Eder et al. showed that when strain was kept constant, relaxation of the wood cells occurred, see Eder et al. (2008). Though the purpose of the study was not primarily to study these effects, the tests show that the cell wall material in fact has viscoelastic properties.

Regarding the individual wood polymers, some conclusions about the strain rate dependence might be drawn on basis of their respective molecular structure. As previously discussed, the amorphous polymers hemicellulose, lignin and amorphous cellulose have a certain transition temperature above which the material softens. The transition temperature is known to increase with increasing strain rate. This means that an amorphous polymer, which is in the softened state, can show brittle fracture when exposed to high strain rates, see Roland (2006). This effect is generally considered to arise from the disordered structure of the amorphous polymer chains, see Figure 6. The individual molecule chains of amorphous polymers are entangled physically and connected by weak Van der Vaals forces as well as occasional covalent bonds. When this entangled structure is strained in tension, the polymer chains tend to straighten out and arrange in parallel to the load. This is a time demanding process and at very high strain rates, brittle fracture can occur before such a rearrangement of the structure takes place. Crystalline polymers, on the other hand, are not entangled in the same way as amorphous polymers. They already possess an ordered structure,

meaning that the behaviour is not influenced by the untangling phenomena, see Figure 6.

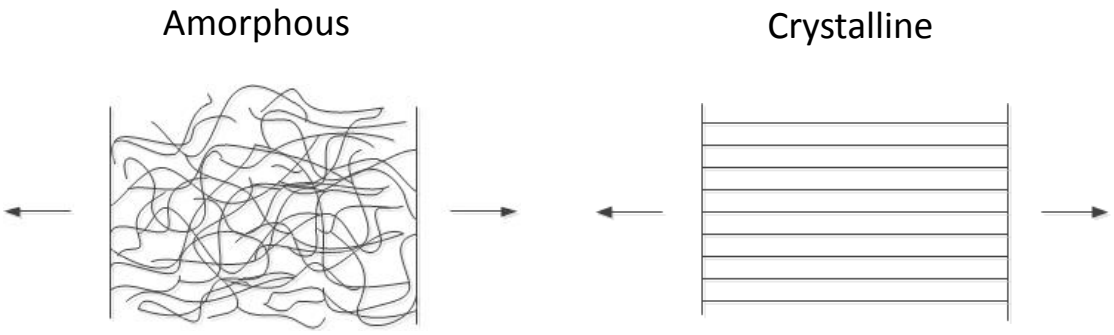

Figure 6 *Schematic illustration of an amorphous (left) and a crystalline (right) molecular structure corresponding to lignin-hemicellulose matrix and cellulose reinforcement respectively*

Therefore, due to the difference in molecular structure, it can be anticipated that the crystalline parts of cellulose show little strain rate dependence, while the amorphous lignin and hemicellulose are likely to be greatly influenced by strain rate.

In the field of plastics, the strain rate influence on yield strength, elastic modulus and fracture characteristics of amorphous polymers is widely known. Plastics often consist of amorphous polymers and show a mechanical response which is greatly dependent on temperature and strain rate. Since there is a lack of data, describing the strain rate dependence of hemicellulose and lignin, experimental data from plastics could possibly be used as approximate values in modelling. Alternatively, macro-level tests on wood could be used for this purpose. For instance, the previously presented compression tests of wet spruce at high strain rates could be used.

Summary

- Data regarding elastic properties and densities of the wood polymers is available in literature (see Table 2 and Table 3). The values are however uncertain for hemicellulose and lignin, especially for the soft state. Yielding and strength properties of the individual wood polymers were scarcely found in literature.
- Cellulose is by far the stiffest and strongest component of wood. It does not soften at high temperatures and moist conditions. Hemicellulose and lignin, on the other hand, are weaker and greatly affected by changes in moisture and temperature.
- The softening behaviour and strain rate dependence of the wood polymers is related to the molecular structure of the polymers. The amorphous wood polymers, i.e. hemicellulose and lignin, are likely to be strain rate dependent whereas the crystalline cellulose is probably less dependent on strain rate.
- No data describing the strain rate dependence of the individual wood polymers were found in literature. However, for wood in the macro-scale strain rate effects have been observed.

2.3 The Steam explosion process

Steam explosion is a method to decompose wood and other biomass into smaller components. The process involves both mechanical and chemical degradation of the wood, Tanahashi (1990). The produced pulp can be used either for production of fibre boards and paper, or in the production of biofuels such as ethanol. In later years, steam explosion has become of increasing interest as an energy efficient alternative to conventional pulping techniques where wood is milled or grinded, or dissolved by chemical means.

In paper and fibreboard production, the goal is mainly to produce a pulp of separated wood cells which have good flexibility and bonding properties. A problem in paper production is that steam explosion pulp often has a rather course structure and dark colour which is unsuitable for paper production, Kokta and Ahmed (1998). In biofuel production, steam explosion is used as a pre-treatment to increase the availability for enzymes to digest cellulose and hemicelluloses into basic sugar units. The sugars can then be converted into ethanol or other biofuels. For this purpose, steam explosion serves to increase the specific area of the cell structure by separating cells, increasing porosity of cells and causing fracture of the cell walls, see Figure 7.

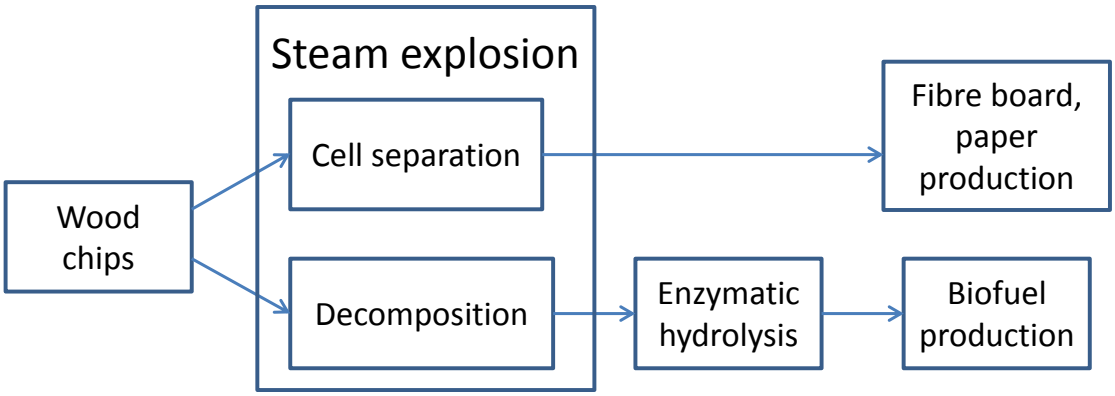

Figure 7 The uses of steam explosion

In the process, wood chips are cooked with high pressure saturated steam at temperatures around 200°C, for a few minutes. During this time, steam permeates the cell structure and the pressure and temperature is distributed more or less equally inside and outside the pore systems of the wood chips, see Figure 8 a. In the next step, the surrounding pressure is released instantly to atmospheric pressure. This causes water inside the pore system to evaporate and expand rapidly, see Figure 8 b-c, Grous et al. (1986).

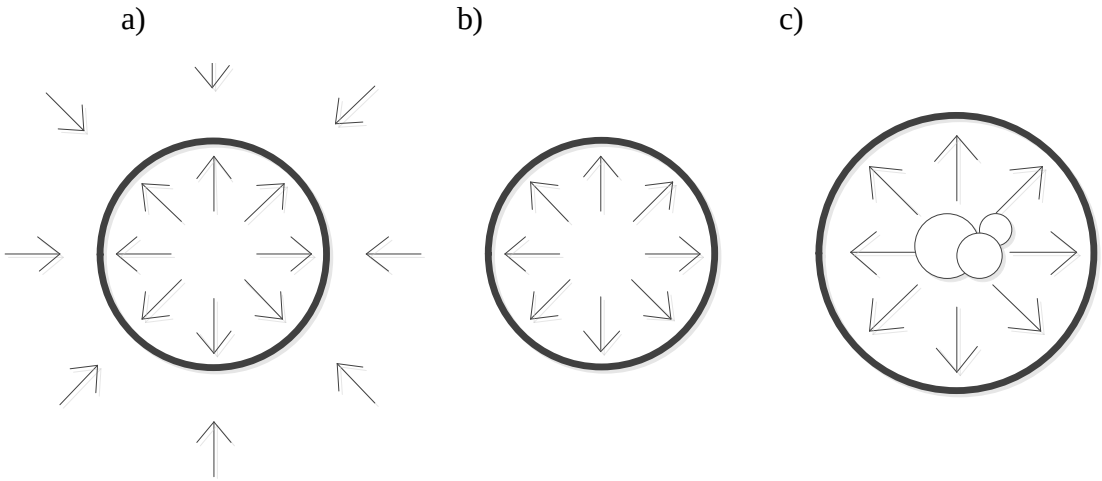

Figure 8 *Simplified drawing of the explosion step in steam explosion. a) before pressure release - pressure is equal outside and inside the pore system, b) just after pressure release - pressure is higher in the pore system than in the surroundings, c) vaporisation occurs inside the pore system*

A lot of effort has been aimed at determining optimal conditions regarding cooking time, temperature, pressure and initial chip size in order to maximise the glucose yield in subsequent enzymatic hydrolysis, see e.g. Grous et al. (1986) and Ballesteros et al. (2000). However, the physical aspects of the sudden decompression of the wood chips seem to be rather little investigated. As vaporisation occurs inside the cell structure, the pressure increases and water and steam is thus pressed out of the wood chip at a high rate. The low permeability of the pore system means that flow of steam out of the wood chip is more or less inhibited and thus, the pressure inside the pore system, P_{in}, becomes higher than the outside pressure, P_{out}. A pressure difference, ΔP, develops where,

$$\Delta P = P_{in} - P_{out} \qquad \text{Eq. 1}$$

The build-up of the net pressure is illustrated schematically in Figure 9. It can be seen that the magnitude of ΔP, and the rate at which it changes, is dependent on the magnitude of the initial pressure, P_0, and on how fast this pressure decreases.

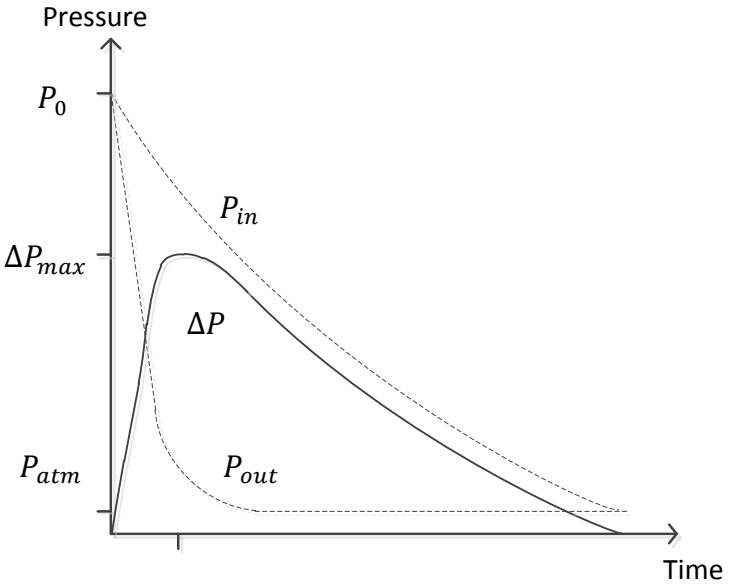

Figure 9 Schematic illustration of the development of the net pressure, $\Delta P = P_{in} - P_{out}$, during the explosion step in steam explosion

The pressure difference causes the cell structure to expand and the strain causes rupture of the cell walls. At the pressure release, the wood chips also collide with each other and with the walls of the reactor vessel. This contributes to the degradation and cell separation of the wood chips, particularly since the lignin middle lamella, which cements cells together, is softened and partly dissolved at the high temperatures present. As the cell structure expands and starts to deteriorate, the porosity and consequently also the permeability increases. This in turn increases the flow out of the pore system and thus decreases the pressure difference.

An investigation of this interplay between pressure, temperature, flow and the porosity of the material is not within the scope of this report. For modelling purposes, we assume that there is no flow and consequently, the load imposed on the cells of the wood chips is considered as an internal pressure, increasing from zero to a maximum value during some time interval. The maximum value of the pressure difference, ΔP_{max}, is assumed to be around 1 MPa and the time interval, Δt_{max}, during which the pressure difference is built up, is assumed to be about 0.01s.

2.4 Wood cell subjected to internal pressure

The wood chips used in steam explosion consist of many wood cells which are cemented together by a lamella consisting mainly of lignin. Before the explosion step, the cells are not generally separated and will interact between themselves. This work was however limited to studying individual isolated cells only and the response of a network of cells is a subject for further research.

As discussed in Section 2.1, the cell can be regarded as a tube with a high ratio of length to width. When present in the wood structure, cells have irregular hexagonal or rectangular cross sections, see Figure 2. The width of the cells might also vary over the cell length. However, if one cell is separated from the structure and inflated by an internal pressure it can be assumed to attain an approximately cylindrical shape. In order for this to be possible, the cell wall material must have sufficient capacity to deform without cracking. Since the wood chips are cooked at high temperature and pressure for some time before the explosion step, it is likely that the material is soft

enough to attain the cylindrical shape. On the other hand, the polymers might be brittle at the high strain rates present.

2.4.1 Principal stresses

For now it is assumed that the wood cell can attain a cylindrical shape. When a cylinder is exposed to internal pressure the principal stresses can be defined in a coordinate system where z, r and φ are the axial, radial and tangential coordinates of the cylinder, respectively. A small piece of material cut out from the cylinder wall is illustrated in Figure 10. The element is approximately flat and is thin in the radial direction meaning that stresses can be assumed to be constant through the thickness of the element.

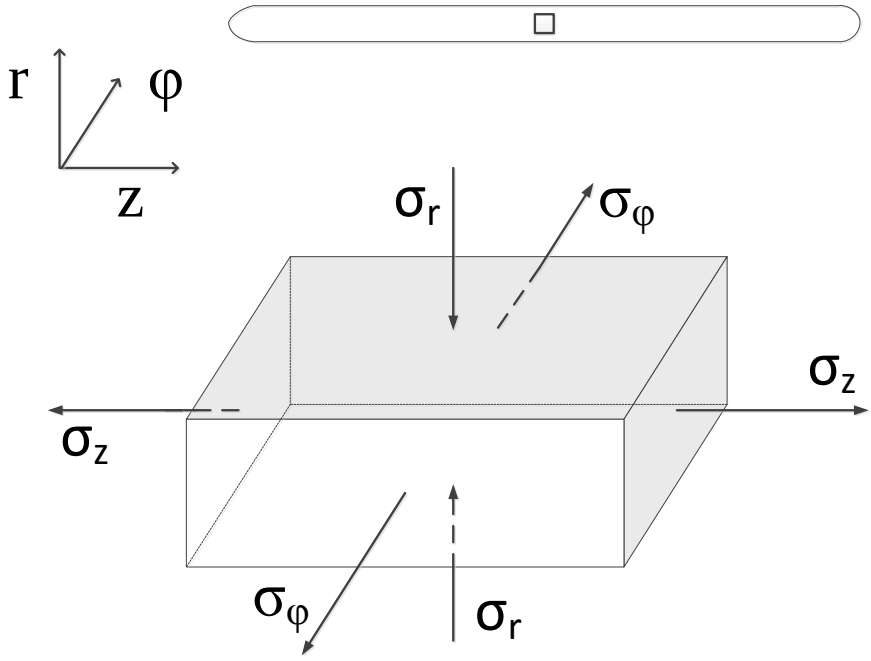

Figure 10 *A small and thin slice cut out from the wall of a cylinder exposed to internal pressure.*

As discussed in Section 2.1, earlywood cells have rather thin walls in relation to the diameter. This means that the assumption of a thin walled cylinder can be made. For such a cylinder the principal stresses caused by an internal pressure are given as

$$\sigma_r = 0 \qquad \text{Eq. 2}$$

$$\sigma_\varphi = \frac{Pa}{h} \qquad \text{Eq. 3}$$

$$\sigma_z = \frac{Pa}{2h} \qquad \text{Eq. 4}$$

where,

σ_r – Stress in the radial direction

σ_φ – Stress in the tangential direction

σ_z – Stress in the axial direction

P – Internal pressure

a – Mean radius of the cylinder

h - Wall thickness of the cylinder

Since the radial stress component, σ_r, is approximately zero, a state of plane stress is assumed for the cell wall. Furthermore, the stress in the tangential direction, σ_φ, is twice as big as in the axial direction, σ_z.

Latewood cells have both thicker walls and smaller diameter than earlywood cells. This means that the thin wall assumption is not appropriate for latewood cells. For a thick walled cylinder with closed ends subjected to internal pressure, the following formulas apply:

$$\sigma_r(R) = \frac{Pr_i^2}{r_0^2 - r_i^2}\left(1 - \frac{r_0^2}{R^2}\right) \quad \text{Eq. 5}$$

$$\sigma_\varphi(R) = \frac{Pr_i^2}{r_0^2 - r_i^2}\left(1 + \frac{r_0^2}{R^2}\right) \quad \text{Eq. 6}$$

$$\sigma_z = \frac{Pr_i^2}{r_0^2 - r_i^2} \quad \text{Eq. 7}$$

where

r_i – Inner radius of cylinder

r_0 – Outer radius of cylinder

R – Radial coordinate ($r_i \leq R \leq r_0$)

Thus, the compressive radial stress goes from $-P$ at the inner face, to zero at the outer face. The tangential tensile stress goes from a maximum value at the inner face, to a minimum value at the outer face and the axial stress is constant through the thickness of the wall. In Figure 11, the through cell wall stress distribution is shown for a cylinder with $r_i = 12$ µm, $r_0 = 15$ µm and $P = 1$ MPa.

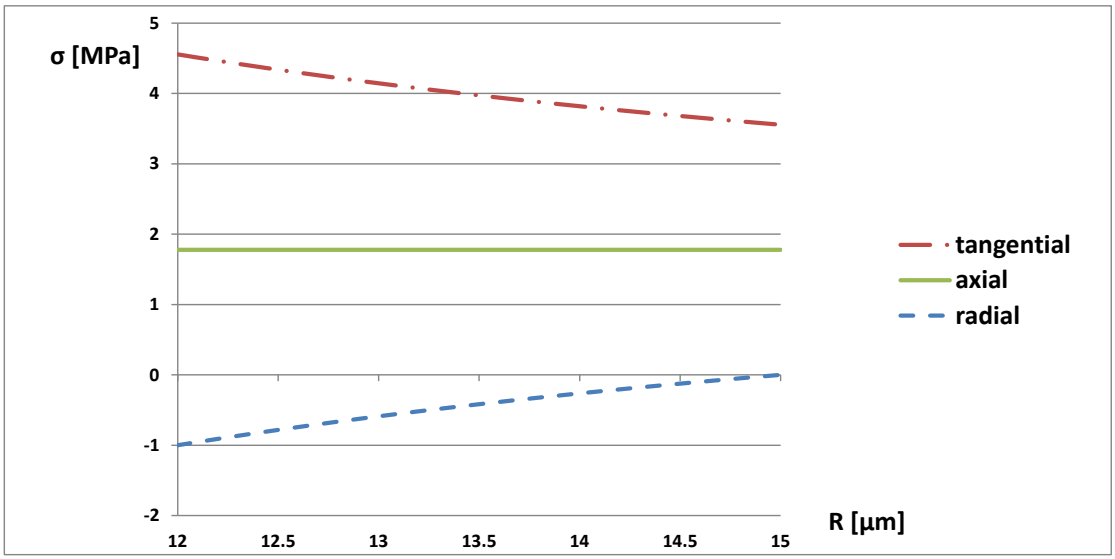

Figure 11 *The stress distribution through the wall of a thick walled cylinder with inner radius 12 and outer radius 15 µm, exposed to an internal pressure of 1MPa.*

The stress distribution shown in Figure 11 applies for a static load. For the dynamic load in steam explosion, the stresses might distribute in a different way for several reasons, e.g. due to inertia effects. For instance, it might be expected when vaporisation occurs locally at some point in the lumen, the nearby cell wall material will initially experience a greater stress than points further away. This might be an important factor since the cells are long in relation to the width. On the other hand, the locally produced vapour will apply pressure on the non-vaporised water which, due to its incompressibility, will efficiently distribute the load to the entire cell.

2.4.2 Internal mechanisms of the cell wall

As discussed in Section 2.1, the cell wall material can be considered as a composite of two components: reinforcement, representing cellulose fibrils; and matrix, representing a mix of hemicellulose and lignin. The different properties of the two components affect the stress distribution in the cell wall when load is applied. If the two materials are given an equal strain, the stress in the reinforcement will be greater due to the greater stiffness. On the other hand, if the two materials are given an equal stress, the strain will be greater in the matrix material due to its low stiffness. Furthermore, the stiffness of particularly the matrix material is likely to be strain rate dependent, see Section 2.2. This means that the stress will be distributed differently for different strain rates.

Mechanism due to microfibril angle

As discussed in Section 2.1, the cellulose fibrils in a wood cell are arranged in a helical pattern around the lumen with a certain microfibril angle, MFA, to the longitudinal axis of the cell. This arrangement of the cell wall, and particularly of the structurally dominant S2-layer, has shown to be an important feature affecting the mechanical behaviour of wood cells. Several studies have been conducted regarding the effect of MFA on the response of wood cells in axial tension.

For instance, Keckes et al. performed tensile tests on individual wood cells and studied these by X-ray diffraction. They observed that the MFA of the cell wall decreased with increasing axial strain of the specimen, see Figure 12. It was

concluded that the helical structure of the cellulose fibrils was elongated as a spring, while the cellulose material in itself had very little strain. The reorientation of the cellulose fibrils gives rise to shear stresses in the matrix material which can cause yielding in shear, either in the interface between matrix and fibril or within the matrix material, Keckes et al. (2003). Furthermore, Eder et al. studied the fracture behaviour of single wood cells, of various shape, loaded in tension. It was observed that the thick walled latewood cells failed by transverse cracking trough the cell, while thin walled earlywood cells failed by buckling due to the helical microfibril structure. This was explained by a tendency for the stiff cellulose fibrils to orient in the main direction of loading, i.e. in the longitudinal direction of the cell which in turn results in torsion of the cell. The tested wood cells were glued to the tensile test device so that rotation of the cell ends was prevented. This resulted in buckling in tension for thin walled earlywood cells, Eder et al. (2008).

Studies of single wood cells exposed to internal pressure were not found in literature. However it can be expected that the same mechanism, i.e. reorientation of the cellulose fibrils in the main direction of stress, occurs also for this type of loading. In the previous section it was discussed how a cylinder exposed to internal pressure experiences axial, tangential and radial stresses in the cylinder wall. For the slender shape of a wood cell, the dominating stress in case of internal pressure is in the tangential direction, see Figure 11. Thus, it can be anticipated that in the case of internal pressure, the cellulose fibrils will tend to orient in the tangential direction, i.e. in the transverse direction of the cell. This would give rise to an increase in MFA and a torsion of the cell as illustrated in Figure 12.

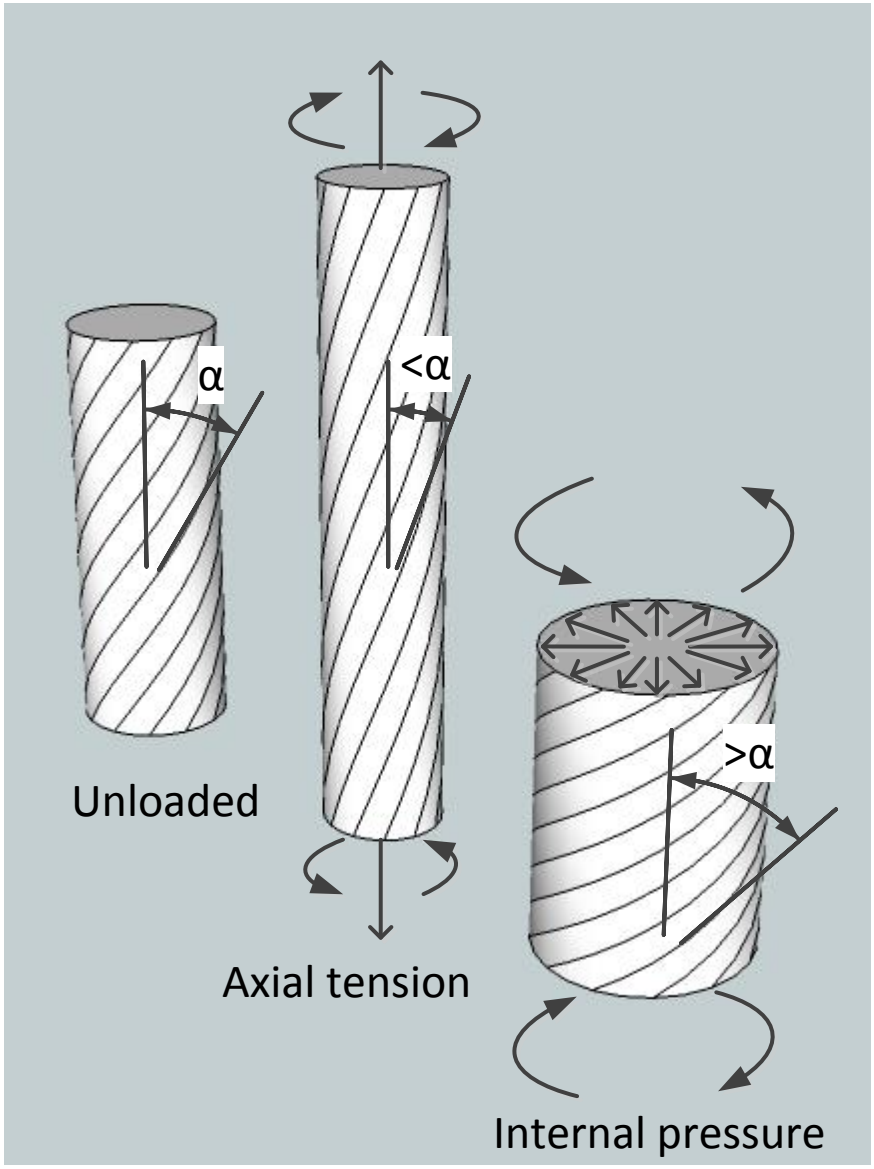

Figure 12 *Segment of a wood cell, modelled as a cylinder with helical reinforcement. The angle, α, of the reinforcement decreases in the case of axial tension and increases in the case of internal pressure.*

Effects of cell wall irregularities

Wood cell walls are in reality not perfect but contain irregularities such as pits and local changes in MFA. Such defects could act as stress raisers and serve as initiation points for failure of the cell wall. Pits, i.e. holes in the cell wall, will force the stress path to change direction, causing a concentration of stresses at the sides of the hole. However, it has been observed that the cellulose fibrils are not interrupted at the pits, but sweep around the opening, so that much of the strength is preserved. The cell wall also increases slightly in thickness around the pit structure, see Kollman and Côté (1968). Even so, Eder et al. found that, for latewood and transitionwood cells in axial tension, pits acted as points of crack initiation. The importance of pits increased with increasing cell-wall thickness and decreasing cell size. For earlywood cells, failure was governed by tension buckling, i.e. collapse of the cell wall due to the helical cellulose fibril structure, Eder et al. (2008).

Possibly, local changes in MFA, as the fibrils sweep around a pit structure or at other points in the cell wall, can act as initiation points for cracks. This was observed by Fernando and Daniel who studied the influence of thermo-mechanical pulping (TMP) on Norway spruce wood. In the TMP process, wood chips are treated by heat and a crushing and grinding action. The ultrastructural changes of the fibres were studied by electron microscopy. It was found that splitting and opening of the cell-wall structure occurred, almost exclusively, along the micro fibril direction. Initiation of cracks could be seen near pits and areas where the micro fibril angle made an abrupt change, Fernando and Daniel (2004).

Strain rate effects on internal mechanisms

For high strain rates, the matrix material can be expected to show higher stiffness and strength than for static loading. The reinforcement material, on the other hand, is likely to be less affected by strain rate due to its crystalline structure, see Section 2.2. This means that the matrix and reinforcement materials should become more equal in stiffness and thus the cell wall should behave more homogeneously with increasing strain rate. The torsional mechanism due to the helical structure of the reinforcement should then be of less importance for the deformation of the cell wall. As the stiffness and strength of the matrix is increased, more reinforcement failure can be expected for high strain rates. The same phenomenon is observed for concrete, where an increased strain rate leads to an increased amount of aggregate failure, Leppänen (2004).

2.5 FE-modelling of wood at the cell wall level

Wood has been studied extensively by finite element analysis in order to determine which factors influence strength, stiffness, moisture related shrinkage and swelling etc. Modelling at the cell wall level has mainly been aimed at deriving properties of wood in the macro scale from the properties of the microstructure, see e.g. Astley et al. (1998) and Qing and Mishnaevsky (2009).

Modelling has also been used to study the mechanical response of wood cell structures in mechanical pulping for paper production. In the process, wood is fed between two discs which rotate at high speed in opposite directions. The wood is thereby exposed to combined shear and compression in the radial direction (see Section 2.1), Persson (2000). To study the deformation of the wood and the decomposition into individual fibres, finite element models of wood cell structures have been used by, e.g.: De Magistris (2005), Holmberg (1998) and Persson (2000). The models are based on homogenisation of the microfibril structure into orthotropic lamellae, representing the various layers of the cell wall.

For instance, De Magistris (2005) modelled a cellular network of a few cells loaded in combined compression and shear transverse to the fibre axis. Properties of the individual wood polymers were used to calculate orthotropic elastic properties for each layer P, S1, S2 and S3 of the cell walls in the system. The properties were defined in relation to the respective micro fibril angle of each layer. A model was then created consisting of layers of elements with anisotropic properties, De Magistris (2005).

In addition to the cell structure models, Persson used the finite element method to firstly determine the collapsed shape of individual wood cells subjected to radial compression and shear, and secondly to determine mechanical properties of the collapsed cells in order to achieve a better understanding of the mechanical behaviour of fibre networks such as papers. By using 2D models, different cross-sectional

shapes of individual collapsed cells were achieved. The cross-sections were then used in 3D-models of wood cell segments to study the response to various types of loading and changes in moisture conditions. Also here, orthotropic lamellae were used to model various cell wall layers. The 3D-models consisted of shell elements with two layers representing S2 and S3 respectively and a third layer representing a combination of S1, P and M. Each layer had orthotropic properties defined in relation to the microfibril angle of each layer. Among the results, a torsional twist upon axial strain, due to the helical winding of the S2-layer, could be observed, Persson (2000).

Despite the high loading rate in the mechanical pulping process, the FE-models created to simulate the process have been static and have not included strain rate dependence of the materials. According to Uhmeier and Salmén (1996), the strain rate in rotating disc refining is about 10^4 s^{-1}. The same authors also showed that the behaviour of wood in compression is highly strain rate dependent (see Figure 5), Uhmeier and Salmén (1996). Therefore, it seems likely that including strain rate dependent properties of the materials would significantly influence the results of these models.

In order to study the internal mechanisms of the cell wall, and their strain rate dependency, it is also desirable to model the micro fibril "reinforcement bars" separately. By doing so, it is possible to distinguish between matrix and fibre failure and to assign different materials with different strain rate dependency to the two components. The problem is that the cellulose fibrils are very finely distributed and modelling a wood cell including the exact microfibril structure would give a very large amount of elements.

To overcome these difficulties, multi-scale modelling can be applied. Saavedra Flores et al. used this approach to study the yielding behaviour of the cell wall. Starting from the basic wood polymers, representative volume elements, RVEs, were created, first of the cellulose fibril, consisting of crystalline and amorphous cellulose, and then of a microfibril consisting of a cellulose fibril embedded in a hemicellulose-lignin matrix. The microfibril-RVE was then used to model the cell wall of a compression wood cell. Compression wood is formed in a part of a tree where compression forces act and wood cells from such regions are characterised by a relatively high microfibril angle in the S2-layer and relatively low cellulose content. Only the S2-layer was modelled since it was considered sufficient for describing the overall behaviour of the cell wall. The model recognised the time dependent behaviour of the lignin-hemicellulose matrix material and a visco-elastic/visco-plastic material model was used for these materials. The analysis was however only carried out at low strain rate. The model was found to, rather accurately, mimic tensile tests of individual wood cells, Saavedra Flores et al. (2011).

3 Modelling in LS-DYNA

In Section 2.4 the response of a single wood cell to steam explosion and the mechanism arising from the helical structure of the cellulose fibrils was discussed. To study these phenomena, a simple model was developed, using the knowledge gained from the literature study. To see how the load effects and mechanism depend on certain parameters, a number of simulations were performed with different values of those parameters. It was also discussed in Section 2.4.2 how the mechanism and load effects are likely to be depending on strain rate due to the strain rate dependence of the cell wall polymers. Due to lack of data, strain rate dependence of the materials was not included in this simple model. However it was a second purpose of the modelling to examine what the magnitude of strain rates might be in the case of steam explosion.

3.1 The model

A model of a single wood cell was created and used to study the deformation mechanisms and the strain rates involved in steam explosion. Single wood cells are the building blocks of the wood chips that are subjected to steam explosion and are not generally separated from the wood chip structure before the explosion step. However, it was the purpose here to study the mechanism arising from the complex structure of the cell wall and not to study the response of an entire wood chip. Therefore the model was limited to only one wood cell, which was considered to be separated from, and acting independently of, the larger wood chip structure.

In Section 2.2, the strain rate dependence of the wood polymers was discussed. The magnitude of strain rate is dependent on the loading rate and on the properties of the different materials. Data describing the relation between strain rate and material properties, such as stiffness and strength, was not found explicitly in literature for the wood polymers. Therefore, a model taking these effects into account could not be directly implemented. Instead the model presented in this chapter uses static material properties, i.e. properties defined to be constant for all strain rates. However, it should be remembered that a strain rate dependent material will give rise to different strain rates than a non-strain rate dependent material. Therefore, the results from this model should only be taken as an indication of what the strain rates might be.

3.1.1 Geometry and mesh

The geometry of wood cells is discussed in Section 2.1. The length of a cell varies between 3-4 mm, the width between 20-40 µm and the wall thickness between 1.7-4.4 µm. The smaller width and greater cell wall thickness correspond to latewood cells while the greater width and smaller thickness applies for early wood cells. The cross-section shape of a wood cell is generally rectangular or hexagonal but was in the model approximated as circular, as discussed in Section 2.4. The model dimensions were chosen to correspond to a transition - late wood cell.

Wood cell walls are built up by the layers P, S1, S2 and S3 which differ in thickness, microfibril angle and chemical composition, see Section 2.1. This model considers only the structurally dominant S2-layer. The S2-layer contains about 50% cellulose, 27% hemicellulose and 23 % lignin. The microfibril angle, i.e. the angle of the cellulose fibrils to the longitudinal axis of the wood cell, of the S2-layer varies between earlywood and latewood but also between juvenile and mature wood, see

Section 2.1. The microfibril angle was in the model set to about 12°, corresponding roughly to a juvenile late wood cell. All the geometric properties used in the model are presented in Table 4.

A cylinder shaped mesh consisting of 40 elements in the circumferential direction and 600 elements in the longitudinal direction was created. The ends of the cylinder were kept open. Use of symmetry was made difficult by the helical structure of the cellulose fibrils and thus, the entire cell was modelled. Simple, 4-node, Belytschko-Tsai shell elements were used which means that only in-plane element stresses were given by the simulations. All elements had the same dimensions of 2 µm in the circumferential direction and 5µm in the longitudinal direction. The thickness of the elements was set to 3 µm which corresponds to the thickness of the cell wall. Each element had two through thickness integration points.

The mesh was divided into a matrix part, representing a mix of hemicellulose and lignin, and a reinforcement part representing cellulose fibrils. The two parts were defined by selecting elements in a helical pattern around the cylinder so that the angle of the helices to the longitudinal axis would roughly correspond to the micro fibril angle chosen for the model, see Figure 13. In reality, the cellulose fibrils are very finely distributed in the cell wall, while in the model, they were bundled into a total of ten helices separated by an equal number of matrix helices. The equal proportions of matrix and reinforcement material in the model is however in accordance with the real case.

Table 4 Geometric properties of the model

Radius [µm]	Length [µm]	Wall thickness [µm]	% Reinforcement	% Matrix
13.5	3000	3	50	50

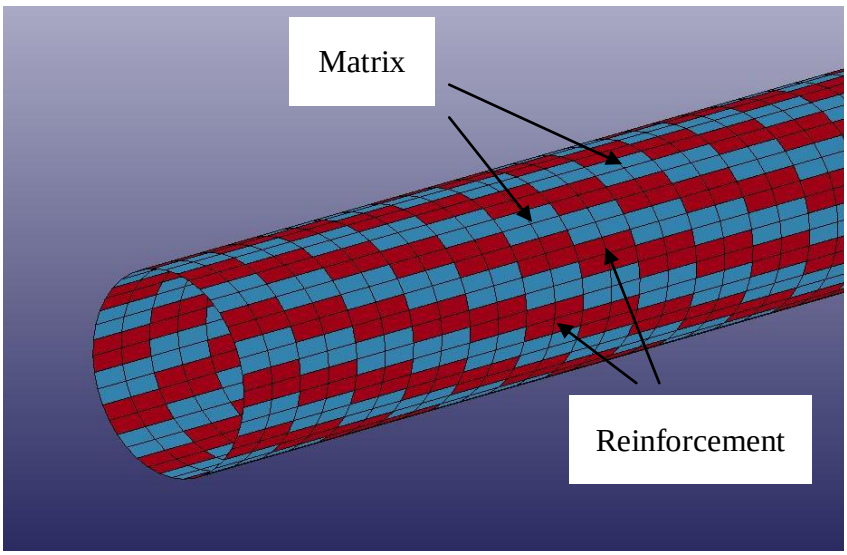

Figure 13 One end of the cylinder mesh used for the model of a single wood cell. The matrix and reinforcement parts are shown in different colours. The thickness of the shell elements are not shown in the figure

3.1.2 Constitutive relation

Separate constitutive relations were employed for the reinforcement and matrix parts. For the reinforcement part, which represents cellulose microfibrils, an ideally elastic material of relatively high stiffness was used. The matrix part, representing a mix of lignin and hemicellulose, was assigned an elastic-plastic material model with relatively low stiffness and yield stress, see Figure 14. Thus, it was assumed that in the real case, the matrix material would yield before failure of the reinforcement material.

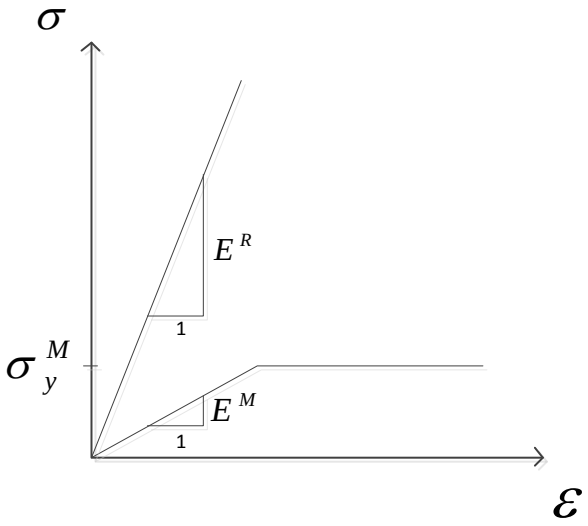

Figure 14 Schematic illustration of the constitutive relation for the reinforcement (R) and matrix (M) material respectively

For the elastic material model used for the reinforcement, three material constants had to be defined: density, Young's modulus and Poisson's ratio. For the elastic-plastic material model used for the matrix, in addition to these three properties, also a yield stress had to be defined.

Values of Young's modulus for the two material models were based on the data recommended by Salmén (2004), see Table 3 of Section 2.2. According to this data, each of the wood polymers: cellulose, hemicellulose and lignin have certain orientations in the cell wall and thus have anisotropic properties. However, it was intended in this model to use a geometric representation of the anisotropy of the cell wall, rather than a material representation. Thus, in this model, isotropic material constants were used for both the reinforcement and matrix material.

The values given for the x-direction, i.e. along the microfibril, of each material were used as isotropic material constants in the model. Due to the moist conditions and high temperatures present in steam explosion, the matrix material was assumed to be in a soft state. For lignin in the soft state, there was a lack of data regarding Young's modulus. For that reason the value given for hemicellulose under wet conditions was used to represent the entire matrix material. At high temperatures, this value can be expected to be even lower than what is given for hemicellulose in the wet state. To study the influence of a reduced matrix stiffness, a second setup with the reference values reduced by 50% was also defined and used in simulations, see Section 3.2.

For the elastic-plastic matrix material model, a yield stress had to be defined. For this purpose, the ultimate strength data presented by Eder, Stanzl-Tschegg and Burgert

(2008) for single wood cells was used, see Section 2.2. To approximate the yield stress of the matrix material, the tensile strength value for an entire wood cell was scaled on basis of the Young's moduli of the reinforcement and matrix materials according to

$$\sigma_y^M = \sigma_u^c \frac{E^M}{E^R} \qquad \text{Eq. 8}$$

where,

σ_y^M – Yield stress of the matrix material,

σ_u^c – Ultimate tensile strength of a latewood cell wall,

E^M – Young's modulus of the matrix,

E^R – Young's modulus of the reinforcement.

Using the Young's modulus for hemicellulose in the wet state, a value of $\sigma_y^M = 0.1194$ MPa was achieved from Eq. 8. It should be noted that using the Young's modulus of hemicellulose in the dry state gives a value of $\sigma_y^M = 11.94$ MPa which is near the value of 11 MPa proposed by Keckes et al. (2003) as the yield stress of the matrix material.

Thus, for the yield stress of the matrix material, a value of $\sigma_y^M = 0.1194$ was adopted. Also here, a second value of the yield stress was calculated and used in the simulations. The second value was also calculated according to Eq. 8, but using the reduced elastic modulus thus resulting in a 50% reduction also of the yield stress.

The two sets of material constants used in the simulations are shown in Table 5.

Table 5 Material constants used for the reinforcement and matrix materials in the simulations 1 and 2

	1	**2**
Reinforcement		
Density [g/cm^3]	1.5	1.5
Poisson's ratio [-]	0.1	0.1
Young's modulus [GPa]	134	134
Matrix		
Density [g/cm^3]	1.5	1.5
Poisson's ratio [-]	0.2	0.2
Young's modulus [GPa]	0.02	0.01
Yield stress [MPa]	0.1194	0.0597

3.1.3 Load

As discussed in Section 2.3, the load imposed on a wood cell in steam explosion can be characterised by a rapidly increased internal net pressure. In reality, both an internal and an external pressure is present during the explosion step. The external pressure decreases at a faster rate than the internal pressure causing a pressure difference, $\Delta P = P_{in} - P_{out}$, to develop, see Section 2.3 and Figure 9. In the model, only the net pressure was applied, i.e. the external pressure was considered to be zero and the internal pressure was equal to ΔP.

The pressure was applied in the direction normal to each shell surface, see Figure 15. This means that the load direction follows the displacement of the element which can cause problems for very large deformations. However, when deformations are small, this definition of the load should give reasonable results.

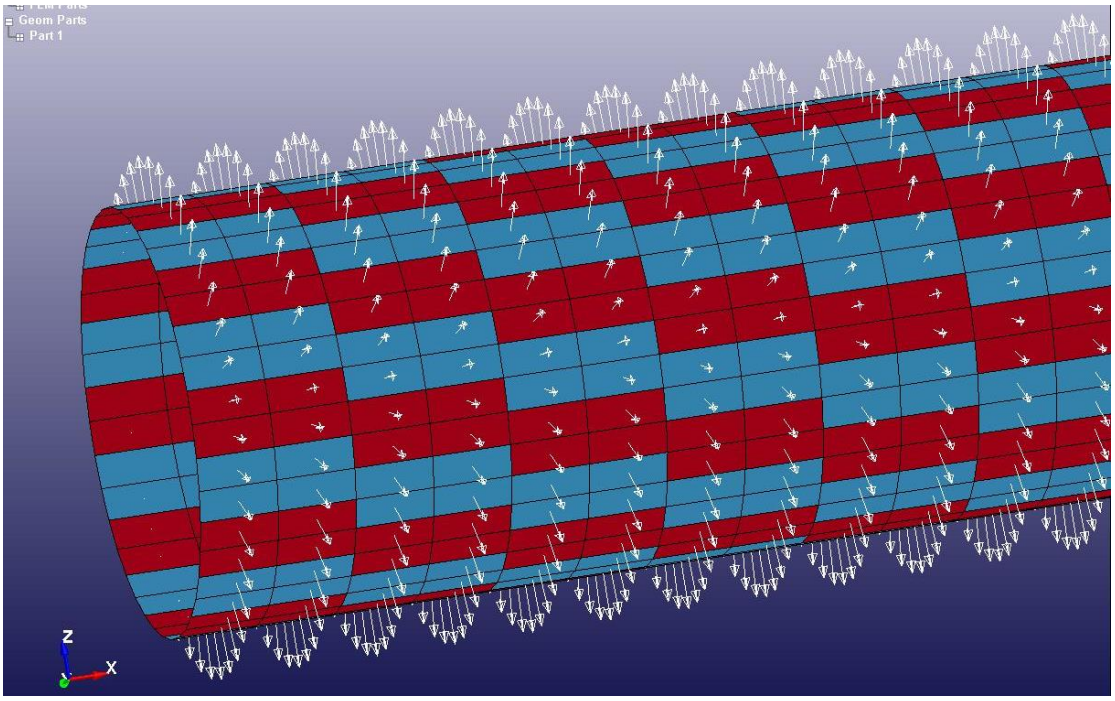

Figure 15 The model with the applied pressure load displayed with arrows

The magnitude of the pressure was defined as a function of time by a load curve. In reality, ΔP increases nonlinearly from zero to a maximum value, see Figure 9. The nonlinear curve was in the model approximated by a linear curve, going from zero to a maximum value, P, on a time interval, Δt. By changing the value of the maximum pressure while keeping the time interval constant, different loading rates, $P/\Delta t$, were achieved.

As a reference setting, $P = 1$ MPa and $\Delta t = 0.01$ s was used. To study the influence of loading rate, two additional load curves were defined with maximum pressure values of $1.1P$ and $0.9P$ respectively, see Figure 16.

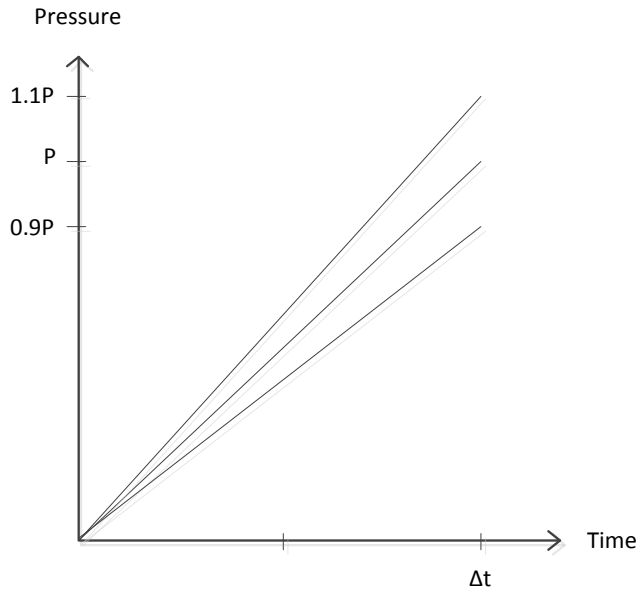

Figure 16 The three different load curves used in simulations

3.1.4 Boundary conditions

In reality the wood cells constituting a wood chip are not separated before the explosion step, see Section 2.3. However in the model, the wood cell was regarded as being isolated and acting independently of the larger wood chip structure. The model was thus assumed to be "floating freely" in space. To prevent large rigid body motion, which can cause problems in the solution, the nodes of the mid-section of the model were constrained against longitudinal translation. This was found to be sufficient to prevent rigid body motion in all the performed simulations.

3.2 Simulation scheme

Using the same model, but with varied material properties and load, several simulations were performed. As shown in Table 5, two sets of material properties were used. The first set represented reference stiffness and strength of the reinforcement and matrix materials. In the second set, the values of the matrix material constants were reduced by 50%, see section 3.1.2. For each set of material properties, three different values of maximum load were used. A reference load, P, was defined and simulations were made with maximum loads of P, 1.1*P and 0.9*P, see section 3.1.3.

Thus, a total of six simulations were performed. The simulations were numbered so that the primary index represents the set of material properties used and the second index represents the load, see Figure 17. A termination time of 3e-4 s was used for all the simulations since it was found to be sufficient to reach yielding in all cases. In order to get the same resolution of the output from the simulations, the output interval was set to 6e-7 s for all the models.

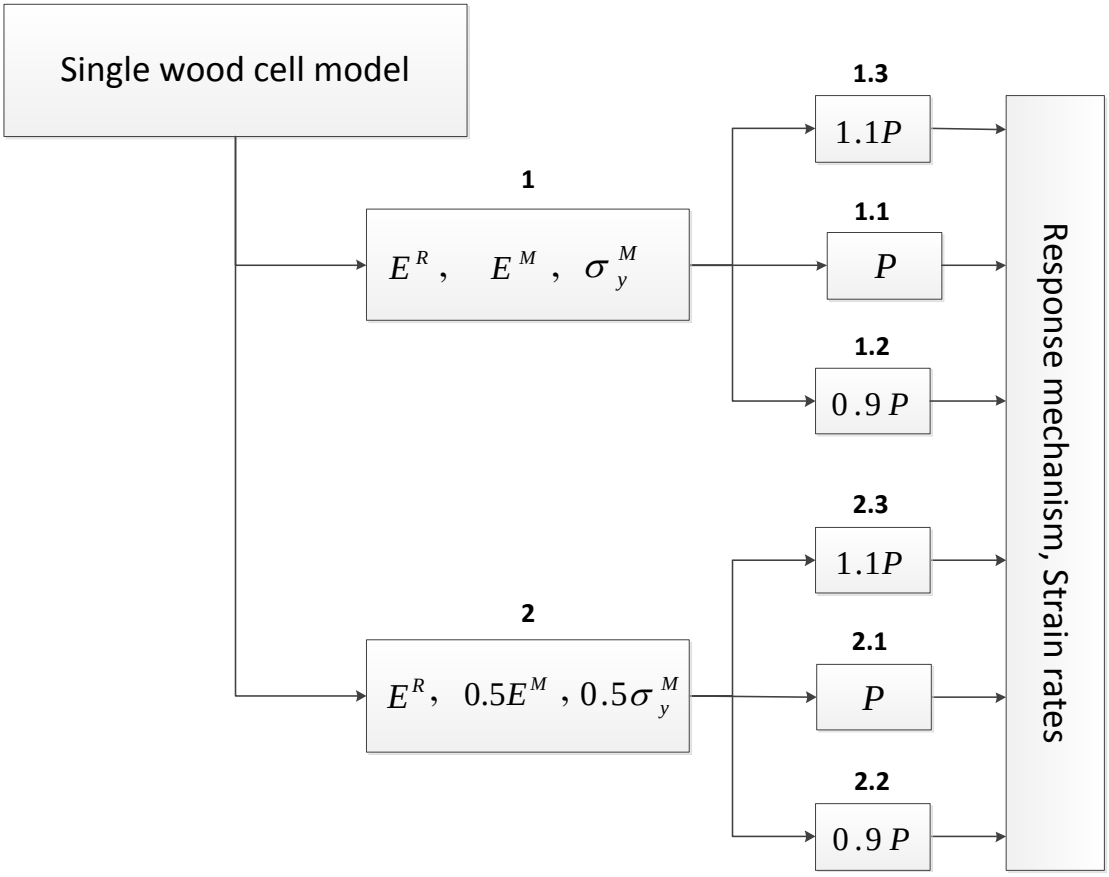

Figure 17 Simulation scheme

3.3 Results of simulations

The shape of the model at t=0 and the deformed shape at t=3e-4 s for the simulation 1.1 is shown in Figure 18. The deformations were greatest at the ends of the model.

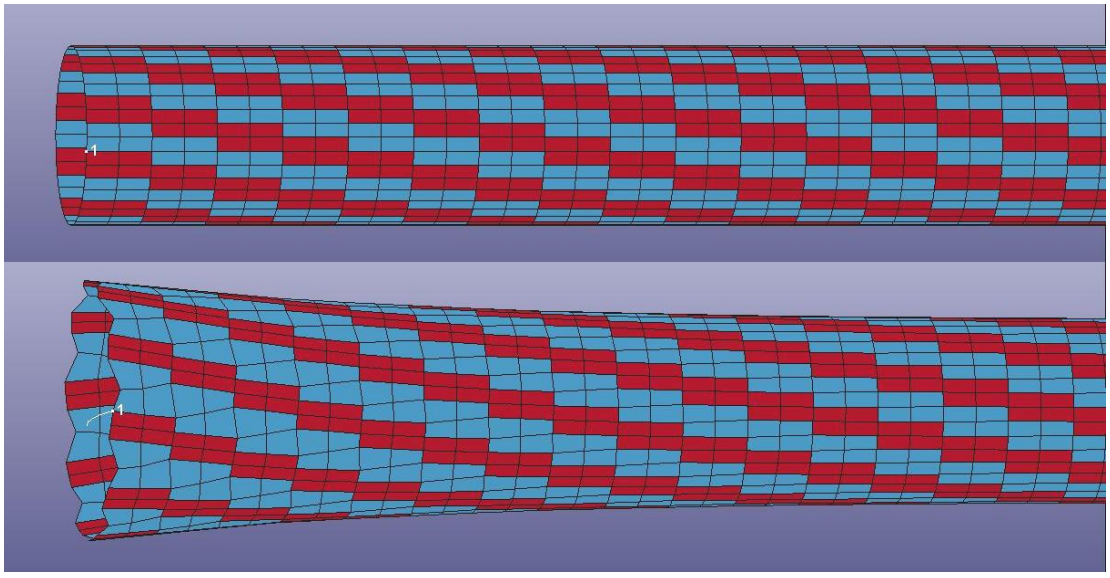

Figure 18 The shape of the model at t=0 and the deformed shape at t=3e-4 s for simulation 1.1

For the simulations with weaker matrix material, very large deformations were achieved which led to instability of the calculations. The simulations were therefore terminated by the program before the specified termination time was reached. This occurred at the times 1.825e-4, 1.996e-4 and 1.685e-4 s for simulation 2.1, 2.2 and 2.3 respectively. Furthermore, since the load was defined in the direction normal to each shell surface, the ends of the model were turned inside out when deformations became large, see Figure 19. Such deformations were considered as unreasonable and were therefore not used for comparison.

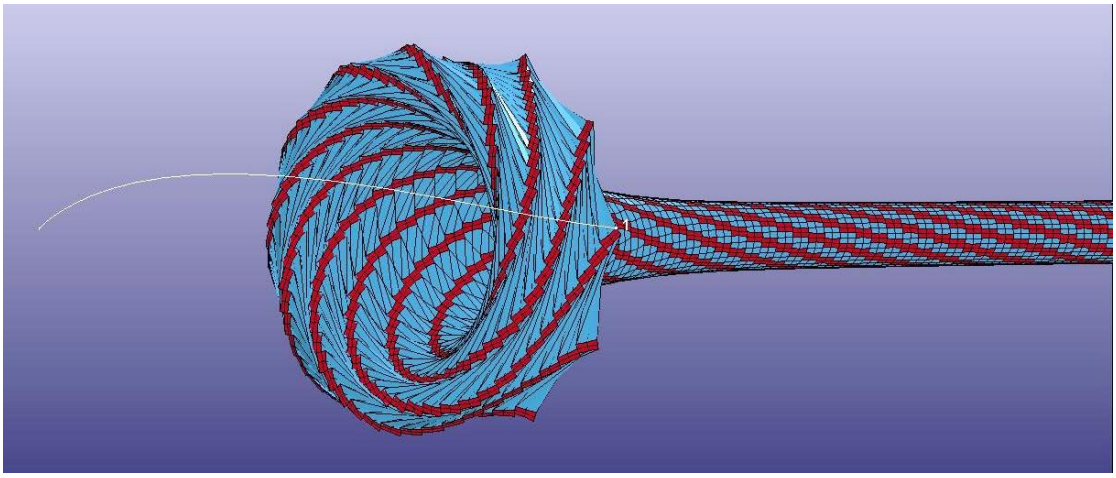

Figure 19 Deformed shape of the model at one end for simulation 2.1 at t=1.656e-4 s

Yielding started at different times for the different simulations, see Table 6. The corresponding yield loads were calculated from the load curve of each simulation.

Table 6 Time of initial yielding and the corresponding load for the simulations

Simulation	Time of initial yielding [s]	Load at initial yielding [kPa]
1.1	2.56e-4	25.6
1.2	2.85e-4	25.7
1.3	2.33e-4	25.6
2.1	1.28e-4	12.8
2.2	1.43e-4	12.9
2.3	1.16e-4	12.8

In order to get a better view of the results, the deformations of the model were transformed to a cylindrical coordinate system defined by a longitudinal (x), radial (R) and angular (θ) coordinates, see Figure 20. The coordinate system has its origin at the left end of the model so that node 1 has an x-coordinate equal to zero in the undeformed model.

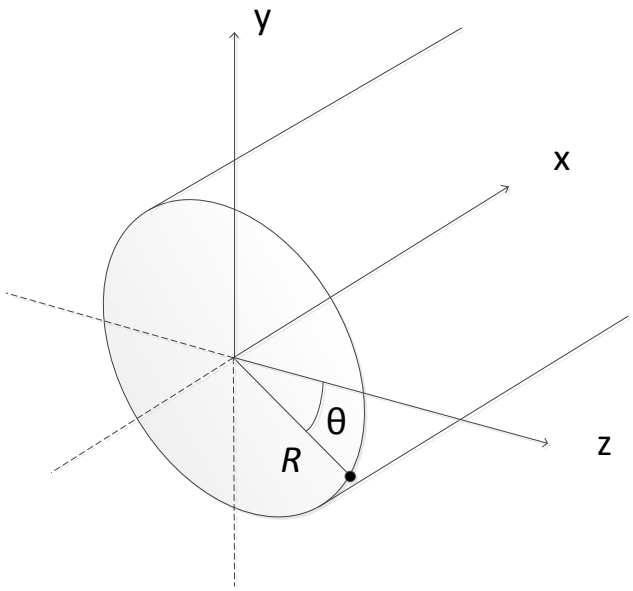

Figure 20 *Definition of the cylindrical coordinate system used for describing deformations*

In Figure 21 and Figure 22 the radial and angular displacements are shown respectively as a function of time for a single node. The node is located between the mid-section and the right end of the model. The simulations 1.1 and 2.1, representing stronger and weaker matrix material respectively, are shown simultaneously for comparison.

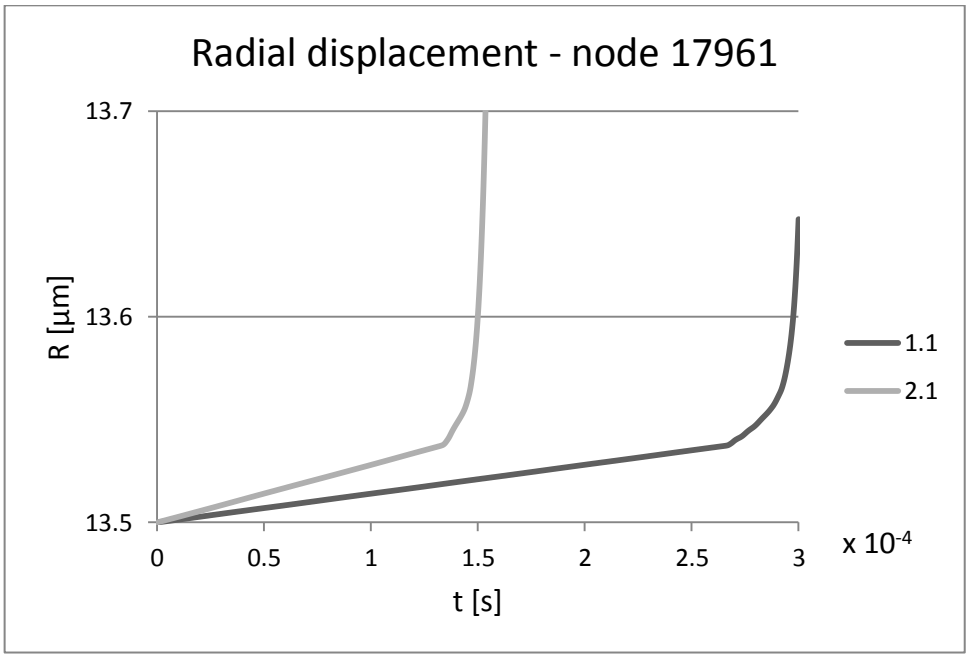

Figure 21 *Radial displacement of node 17961 as a function of time for the simulations 1.1 and 2.1*

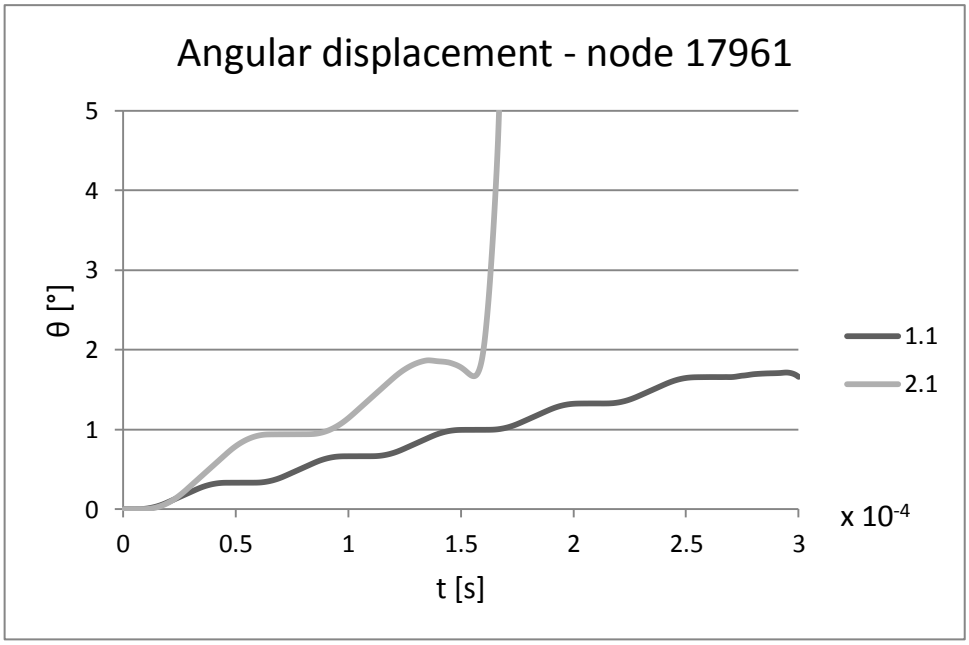

Figure 22 Angular displacement of node 17961 as a function of time for the simulations 1.1 and 1.2

In Figure 23 and Figure 24, the angular and longitudinal displacements at a single time instant, $t=1.5*10^{-4}$ s, are shown as a function of the longitudinal coordinate respectively. Also here, the weaker and stronger matrix material simulations are shown simultaneously.

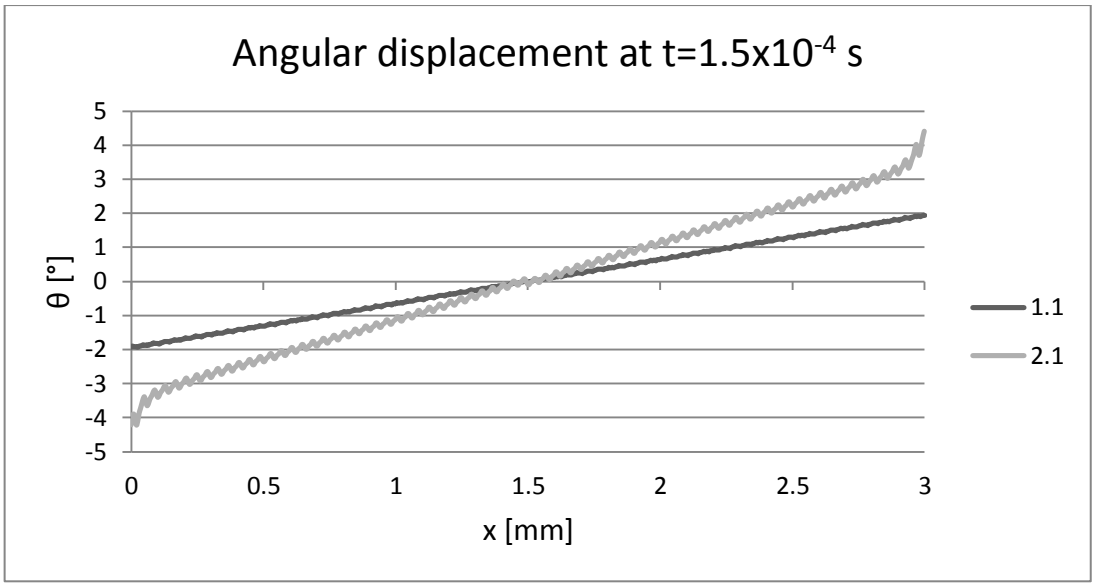

Figure 23 Angular displacement as a function of the longitudinal coordinate at time $t=1.5*10^{-4}$s

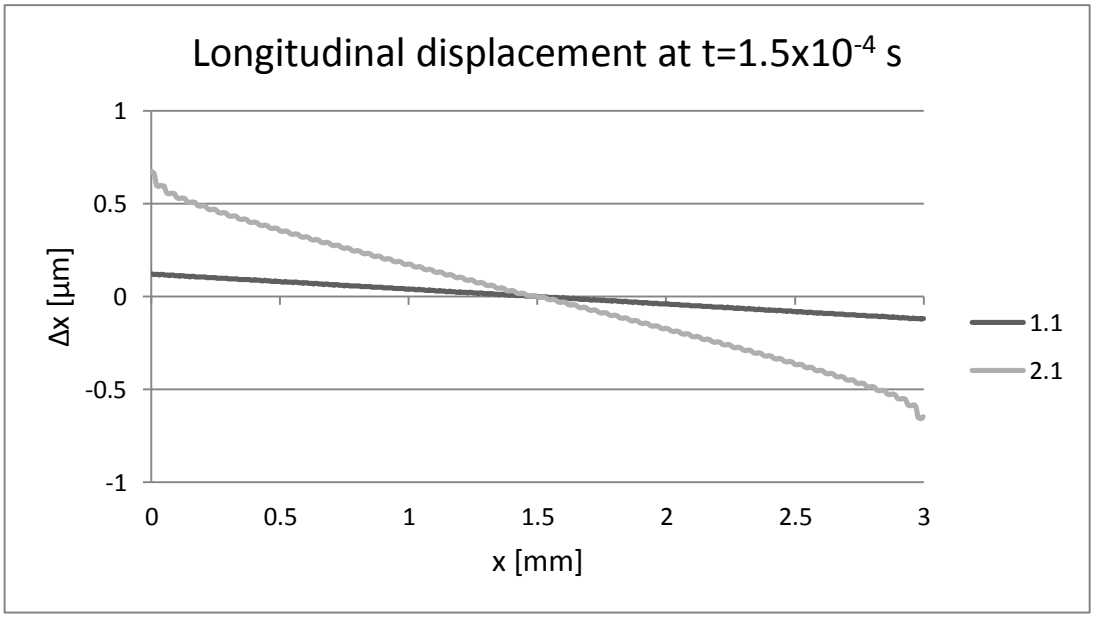

*Figure 24 Longitudinal displacement as a function of the longitudinal coordinate at time 1.5*10^{-4}s*

The strain energy density of a matrix element (element 18000) located between the mid-section and the right end of the model was calculated on basis of the stress and strain tensors given for the element in simulation 1.1. The total strain energy density along with the deviatoric part of the strain energy density is shown in Figure 25.

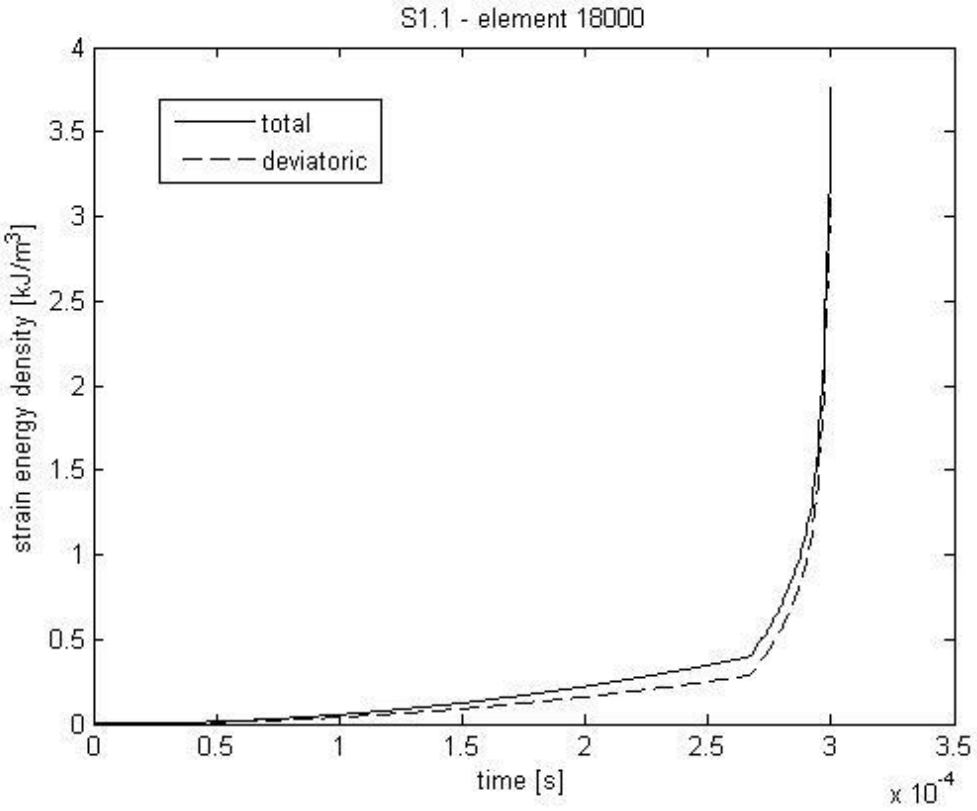

Figure 25 Total and deviatoric strain energy density of a matrix element in simulation 1.1

Effective strain rates were plotted against time for two nodes belonging to the matrix and the reinforcement part respectively. The two nodes were located at the same length coordinate, between the mid-section and the right end of the model. The effective strain rate of the matrix node (node 18000) and the reinforcement node (node 17962) is shown in Figure 26 and Figure 27 respectively. Values of strain rate above 50/s are excluded in the graphs to give a better view of the events before yielding.

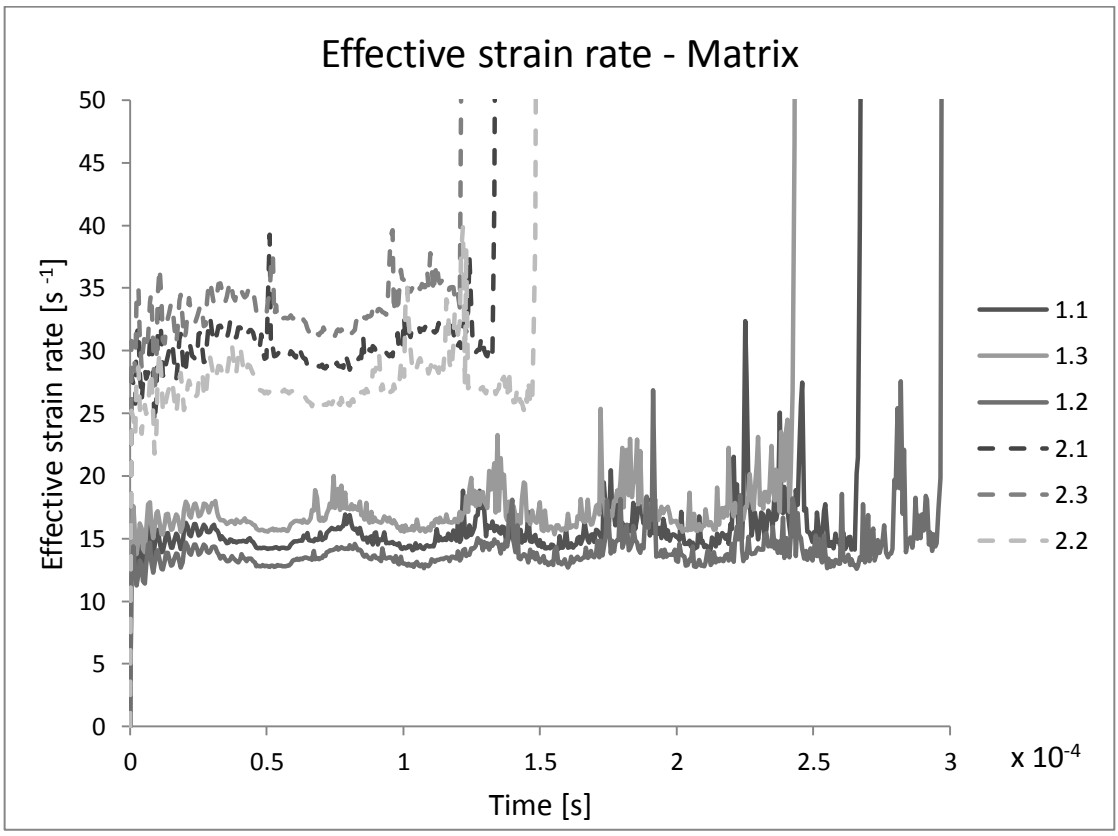

Figure 26 Effective strain rates in the six simulations at a matrix node (node 18000)

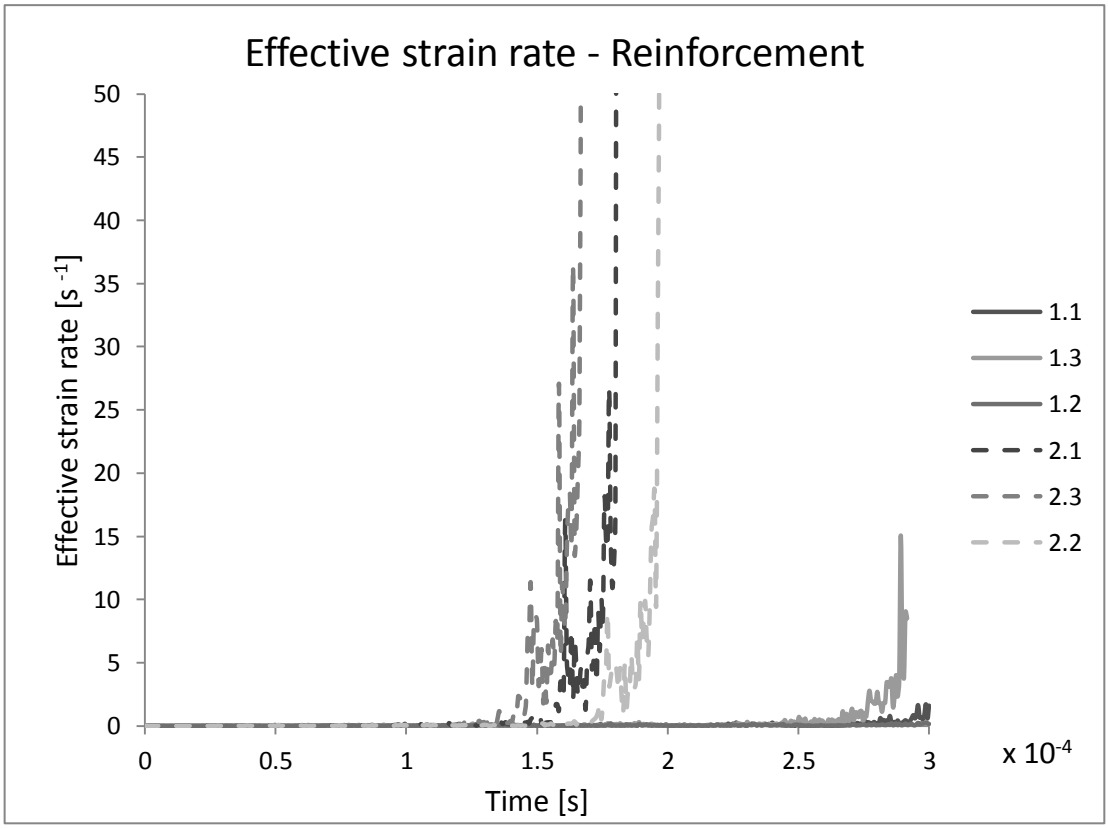

Figure 27 Effective strain rates in the six simulations at a reinforcement node (node 18000)

3.4 Comments on simulation results

In all of the six simulations, a similar deformation pattern can be seen: the cylinder radius increased while the length of the cylinder decreased with increasing load. It can also be seen that the model deformed in a torsional mode, see Figure 22 and Figure 23. In Section 2.4.2, it was discussed how such a mechanism is likely to arise due to the helical microfibril structure. The simulations confirm that the reinforcement strives to orient in the tangential direction of the cylinder. This behaviour was even more pronounced for the simulations with weaker matrix material, see Figure 23. Since the ends of the cylinder were kept open in the model, there was no load acting in the axial direction of the model. If the model had been provided with closed ends, the load acting on the ends would have caused an additional axial stress component which would have counteracted the twisting deformation and served to straighten out the reinforcement.

The rearrangement of the reinforcement gives rise to deviatoric strains in the elements. In Figure 25 it can be seen that the matrix element has mainly deviatoric strain. This is explained by a predominant shear stress and strain of the matrix. In the extreme case of deformation, the reinforcement would be arranged completely in the tangential direction, i.e. with an angle of 90° to the longitudinal axis of the cylinder. For initial angles closer to 90°, much smaller deviatoric straining would be needed to reach this ultimate state. Thus, it could be expected that layers of the cell wall which have higher initial microfibril angles, such as the S1-layer, will fail for loads of lower magnitude than layers of low initial microfibril angle.

For all simulations, yielding of the matrix material started at the elements located at the ends of the cylinder. Due to the regularity of geometry, material properties and

load, yielding occurred simultaneously for all elements around the edge of the cylinder. In reality, yielding would start from some weak point in the structure and cause localised deformation. Such a weak point could be for instance a pit structure, as discussed in Section 2.4.2.

The strain rate histories for a matrix and a reinforcement element, located at the same longitudinal coordinate of the model are shown in Figure 26 and Figure 27 respectively. For the matrix element, the six simulations all show a similar pattern; as long as the material is in the elastic stage, the resistance of the element increases with increasing load and thus the strain rates approach an approximately constant average value, although large oscillations occur. When yielding starts, the resistance of the element cannot increase further and the strain rates thus increase dramatically. Therefore, the greatest strain rate was achieved for the simulation in which yielding was reached first, i.e. in simulation 2.3. In the real case, the material might fail before reaching such high strain rates as were achieved in the simulations.

The strain rates for the reinforcement element are considerably smaller than for the matrix element, see Figure 27 and Figure 26. This is probably due to the much greater stiffness of the reinforcement material. Also for the reinforcement element, a very rapid increase of the strain rate can be seen for times of about 1.5e-4s for the simulations with weaker matrix material, and about 2.7e-4s for the simulations with reference material. Since the reinforcement material was elastic and did not include a yield criterion, this cannot be explained by yielding of the element. Instead it is probably caused by redistribution of load due to yielding of the matrix elements. When all the matrix elements have reached yielding, the matrix part cannot carry anymore load. Thus the load, as it increases beyond this point, has to be carried by the reinforcement.

The simulations confirm that the strain rate is dependent on the material properties as well as on the loading rate of the simulation. The strain rate histories from the simulations with equal stiffness have a similar appearance although the curves are shifted up and down depending on the loading rate. It can also be seen that the difference due to loading rate was greater for the simulations with lower stiffness, i.e. loading rate had a greater influence for those simulations.

4 Conclusions and discussion

The work consisted of a literature review and a modelling part. The main conclusions from the two parts are here presented and discussed separately. Possible subjects for further research are also presented at the end of the chapter.

4.1 Wood cell subjected to steam explosion

In the introduction, a number of research questions were formulated. In this section, it is discussed how these research questions have been answered through the literature review.

What is the structure to be modelled, i.e. the structure of a wood cell?

Softwood cells can have various sizes and shapes depending on cell type and from what part of the tree it comes from. The dominating cell type is the tracheid, which can be characterised as a long, slender tube. The cell wall can be considered as a layered composite structure with long cellulose fibrils, embedded in a matrix of lignin and hemicellulose. Of the various cell wall layers, the S2-layer can be considered as structurally dominant. The helical winding of the cellulose fibrils, particularly in the S2-layer, has been shown to be an important feature of the cell wall.

What mechanical properties of the cell wall should be used?

Elastic properties of cellulose, hemicellulose and lignin are available from experiments, molecular modelling and theoretical estimates. The properties depend greatly upon temperature and moisture. The high temperatures and moist conditions in steam explosion imply that the matrix polymers, hemicellulose and lignin as well as the non-crystalline parts of cellulose are in a soft state before the pressure release.

Due to the problems involved in performing experiments on isolated wood polymers the elastic properties contain a great deal of uncertainty and there is a lack of data regarding yielding and strength properties as well as the strain rate dependence of the materials. For lignin and non-crystalline cellulose there is also a lack of data regarding the elastic properties in the soft state.

The probable existence of strain rate dependence of the amorphous wood polymers, in combination with the high strain rates achieved from modelling with non-strain rate dependent material properties, indicates that a strain rate dependent constitutive relation should be used in modelling wood cells subjected to steam explosion.

How does the material respond to high strain rates?

Strain rate dependence is likely to exist for hemicellulose and lignin since they are polymers with amorphous molecular structure. Experimental data explicitly describing such behaviour was however not found in literature. The cellulose is likely to be less strain rate dependent since it has a more crystalline structure.

Studies of strain rate dependence have been performed on various types of plastics, some of which might resemble the wood polymers in molecular structure. Data for such plastics could potentially be used in a material model describing hemicelluloses and lignin. A model could also be based on experiments on wood in the macro scale.

What are the characteristics of the load in steam explosion?

The action of steam explosion to wood cells involves both mechanical and chemical aspects. At the explosion step, an interplay between pressure flow and expansion of

the cell structure takes place. Impacts also occur as separated wood cells and wood chip fragments collide with each other and with the vessel walls.

In this work, the load imposed on the wood cell was simplified to that of a rapidly increased internal pressure. The response of cells to impact loads is a subject for further research.

Which are the possible determining internal mechanisms?

A particular mechanism arises from the helical structure of the cellulose fibrils. When individual wood cells are strained in axial tension, the fibrils reorient in the axial direction. For a wood cell subjected to internal pressure, the fibrils should instead strive to reorient in the tangential direction since that is then the direction of greatest stress. The reorientation of the fibrils induces shear to the hemicellulose-lignin matrix. For high strain rates, the stiffness and strength of the matrix might be significantly enhanced meaning that the cell wall will behave more homogenously.

How is wood modelled at the cell wall level?

At the cell wall level, wood is often considered as a composite in which cellulose fibrils act as reinforcement embedded in a hemicellulose-lignin matrix. Due to the complex ultrastructure, homogenisation is often applied to simplify the geometry. For instance, the different layers of the cell wall are often modelled as orthotropic lamellae with material properties defined in relation to the microfibril direction of the respective layer. A common approach is to model the S2-layer only, since it is considered as structurally dominant.

Furthermore it is concluded that, in previous FE-models of wood cells, little attention has been devoted to studying strain rate effects.

4.2 Modelling in LS-DYNA

The commercial finite element software LS-DYNA was used for transient analysis of a single wood cell exposed to steam explosion. The created model was very rough and idealised. This makes it hard to draw conclusions from the results about the real behaviour of wood in steam explosion. However, the simulations did show certain interesting phenomena which would be desirable to explore further.

It could be seen that a torsional mechanism was formed due to helical structure of the reinforcement material. This is in line with what has been observed in experiments on wood cells subjected to axial tension. Furthermore, the strain rates achieved from the simulations were very high. This means that introducing a strain rate dependence to the material model is likely to have a significant effect on the output of the simulations. Strain rate dependence is also likely to affect the torsional mechanism.

To be able to explore these phenomena in more detail, the model has to be improved in several ways. Several measures could be taken regarding the geometry, load, boundary conditions and material representation.

Geometry and mesh

The modelled geometry was very simplified and rather far from the actual structure of a wood cell. The model included only the S2-layer of the cell wall. Due to the geometric representation of the helical microfibril structure, including the additional cell wall layers is difficult. To model a multi-layered structure it is necessary to use

eight node elements, i.e. solid or thick shell elements. The orthotropic lamella approach described in Section 2.5 could possibly be applied, although it is uncertain whether such a method is compatible with a strain rate dependent constitutive relation.

In an improved model it would be desirable to also model the end segments of the wood cell. These could be modelled as cones or semi ellipsoids. Complex geometries do however have the disadvantage that small elements might be needed which means that also the time-steps become small. A possibility could be to use a few truss elements to keep the ends together. In this way, the very large radial deformations after yielding could be prevented while rotation of the ends can still take place.

In the performed simulations, yielding occurred simultaneously at the ends of the model. In reality, yielding or fracture will start from some weak point in the cell wall structure. Such weak points could be geometric irregularities such as pits, or local changes in microfibril angle, see sections 2.1 and 2.4.2. In the real case, cellulose fibrils are continuously passing around the pit opening in a sweeping manner, see 2.4.2. Thus, a simple way of representing the pit structure could be to assign a weaker material to a few matrix elements at some point while leaving the neighbouring reinforcement elements intact. This would however not account for the associated change in cellulose fibril angle. A local angle change could simply be made by reselecting the elements belonging to the reinforcement part so that the angle of the helix changes at some point along the length.

It would also be desirable to refine the mesh and make the two parts more continuous. Refining the mesh does however make simulations more costly. To reduce simulation cost it might be possible to use symmetry to model only a part of the cylinder. The deformations given by the performed simulations were symmetric about the mid-section, however the rotation had opposite signs on opposite ends. The rotation at the mid-section was equal to zero. If a cylindrical coordinate system is used, the torsional deformation can be prevented at the mid-section.

Load

For modelling purposes, the loads involved in steam explosion were characterised as a rapidly increased internal net pressure. In the model, the load was defined as an internal pressure only. The magnitude of this pressure was taken as the difference between the internal and the external pressure that wood cells are subjected to in the real case, see Section 2.3. An alternative could be to include both the internal and the external pressure in the model. If solid elements had been used, this would have given a slightly different radial stress through the cylinder wall. However, the shell elements used in this model can only have in-plane stresses and no radial stress is thus calculated. Therefore, the influence of including external pressure to the model would be small.

Boundary conditions

Symmetry boundary conditions could possibly be used to model only half the cell. The nodes of the mid-section should then be prevented from tangential translation while radial translation should be free. Thereby, the mid-section is prohibited from rotating but allowed to expand. Constraints at the ends of the model could be used to represent the closed ends of wood cells without modelling the actual geometry of the end pieces. The nodes of the end sections should in that case be prevented from radial translation while allowing tangential translation. In that way, the ends would be prevented from expanding while being allowed to rotate. This solution will however

be an approximation since the end pieces are not completely rigid in the real case. The axial load coming from the pressure acting on the closed ends could be applied instead to the nodes of the end sections. This load should then be calculated as the internal pressure times the inner cross-section area of the cylinder, divided by the number of nodes of the section.

Possibly boundary constraints could be applied also to represent the conditions when the wood cell is incorporated in a wood chip structure.

Material

In general, the behaviour of the materials under the extreme conditions of moisture, temperature and strain rate needs to be investigated further in order to establish adequate material representation for modelling. Including strain rate dependence to the matrix material would also be desirable. In LS-DYNA, both the Young's modulus and the yield stress can be defined as functions of strain rate. However, no such data was found in literature for hemicellulose and lignin. Data might be obtained from macro-level tests as discussed in section 2.2 or from materials with similar molecular structure. If stiffness and strength of the matrix material is defined to increase with increasing strain rate, this should make the difference between the reinforcement and matrix material smaller.

In the presented model, the amorphous parts of cellulose which occur periodically along the cellulose fibrils were not taken into account. To represent amorphous cellulose, a third material could be introduced to the model. A failure criterion could be introduced to this material, thus allowing failure to occur also for the reinforcement. Data describing amorphous cellulose is however scarce and the material constants would have to be estimated.

Comparison to experiments

No experiments on the behaviour of single wood cells exposed to internal pressure were found in literature. However, tensile tests of individual wood fibres, such as the ones performed by Eder et al. (2008), could possibly be used for verifying and calibrating the model. In order to simulate the tests, a prescribed axial deformation could be applied to one end of the model, while the other end is locked in the axial direction. Both ends should also be constrained against rotating since this was the case in the experiments.

A comparison between simulations and experimental results could give some indication of whether the overall stiffness and strength of the model and its materials is correct. However, the special conditions in steam explosion, e.g. high temperatures and high loading rate, were not the same in the experiments and thus a different response could be expected. The displacement rates in the tests were low, meaning that no conclusions can be drawn about the behaviour at high strain rates from these tests.

4.3 Further research

The development of the presented model, including the suggested improvements, is a subject for further research. This includes in particular the development of a strain rate dependent material model. Further experimental investigation of the wood polymers might be necessary in order to accomplish this. When the model has been improved and verified by comparison to experimental data, a parametric study can be performed in order to study the influence of certain parameters in the steam explosion

process. It might also be relevant to consider other wood types than softwood and to model impacts of wood cells and the vessel wall.

Modelling could also be made at other levels than that of individual cells. In addition to the single wood cell model presented in this work, it would be interesting to model a network of cells representing the micro-structure of a wood chip. A simplified representation of the cell wall, using the information gained from the single wood cell model, could possibly be used to see how the different cells interact. Such a model could possibly also be used to study the relation between pressure, flow and deformations in the cell structure.

Some of the discussions, models and conclusions made in this work regarding strain rate effects and deformation mechanisms of wood cells, might also be applicable to other processes than steam explosion. For instance, strain rates are known to be high also in mechanical pulping with rotating disc refining and, although the load is different, the same principles could apply. In further research, it would be interesting to establish a transient finite element model to simulate this process. Possibly, the same strain rate dependent material as in steam explosion could be used for this purpose.

5 References

Astley, R.J., Stol, K.A. & Harrington, J.J., 1998. Modelling the elastic properties of softwood. *Holz als Roh- und Werkstoff*, 56(1), pp.43–50.

Ballesteros, I. et al., 2000. Effect of Chip Size on Steam Explosion Pretreatment of Softwood. *Applied Biochemistry and Biotechnology*, 84-86(1-9), pp.97–110.

Barret, J.D., 1981. Fracture mechanics and the design of wood structures. *Philosophical Transactions of the Royal Society of London. Series A, Mathematical and Physical Sciences*, 299(1446), pp.217–226.

Chen, W., Lickfield, G.C. & Yang, C.Q., 2004. Molecular modeling of cellulose in amorphous state. Part I: model building and plastic deformation study. *Polymer*, 45(3), pp.1063–1071.

Cousins, W.J., 1978. Young's Modulus of hemicellulose as Related to Moisture Content. *Wood Science and Technology*, 12(3), pp.161–167.

Dinwoodie, J., 2010. Timber. In *Construction Materials*, eds. P. Domone & J. Illstone, pp. 403-506. New York: Spon Press.

Eder, M., Stanzl-Tschegg, S. & Burgert, I., 2008. The fracture behaviour of single wood fibres is governed by geometrical constraints: in situ ESEM studies on three fibre types. *Wood Science and Technology*, 42(8), pp.679–689.

FAO, 2005. *Global Forest Resources Assessment 2005, Progress Towards sustainable forest management*, Rome.

Fernando, D. & Daniel, G., 2004. Micro-morphological observations on spruce TMP fibre fractions with emphasis on fibre cell wall fibrillation and splitting. *Nordic Pulp and Paper Research Journal*, 19(3), pp.278–285.

Grous, W.R., Converse, A.O. & Grethlein, H.E., 1986. Effect of steam explosion pretreatment on pore size and enzymatic hydrolysis of poplar. *Enzyme and Microbial Technology*, 8(5), pp.274–280.

Holmberg, S., 1998. *A numerical and experimental study of initial defibration of wood*, Phd Thesis, Lund Institute of Technology, Lund, Sweden.

Hoffmeyer P. , 1995. Wood as a building material. Timber Engineering STEP 1, H. J. Blass, P. Aune, B. S. Choo, R. Görlacher, D. R. Griffiths, B. O. Hilson, P. Racher, and G. Steck, eds., Centrum Hout, Almere.

Keckes, J. et al., 2003. Cell-wall recovery after irreversible deformation of wood. *Nature materials*, 2(12), pp.810–814.

Kim, D.-Y. et al., 2001. Thermal Decomposition of Cellulose Crystallites in Wood. *Holzforschung*, 55(5), pp.521–524.

Kokta, B. V & Ahmed, A., 1998. Steam Explosion Pulping. In *Environmentally Friendly Technologies for the Pulp and Paper Industry*, eds. R. Young & M. Akhtar, pp. 191-214. New York: John Wiley & Sons, Inc.

Kollman, F.F.P. & Côté, W.A., 1968. *Principles of Wood Science and Technology, 1. Solid Wood*, Berlin: Springer-Verlag.

Leppänen, J., 2004. *Concrete Structures Subjected to Fragment Impacts*, Phd Thesis, Chalmers University of Technology, Gothenburg, Sweden.

De Magistris, F., 2005. *Wood fibre deformation in combined shear and compression*, Phd Thesis, Royal Institute of Technology, Stockholm, Sweden.

Mindess, S. & Madsen, B., 1986. The fracture of wood under impact loading. *Materials and Structures*, 19(1), pp.49–53.

Mishnaevsky, L. & Qing, H., 2008. Micromechanical modelling of mechanical behaviour and strength of wood: State-of-the-art review. *Computational Materials Science*, 44(2), pp.363–370.

Persson, K., 2000. *Micromechanical modelling of wood and fibre properties*, Phd Thesis, Lund Institute of Technology, Lund, Sweden.

Qing, H. & Mishnaevsky, L., 2009. 3D hierarchical computational model of wood as a cellular material with fibril reinforced, heterogeneous multiple layers. *Mechanics of Materials*, 41(9), pp.1034–1049.

Roland, C.M., 2006. Mechanical Behavior of Rubber at High Strain Rates. *Rubber Chemistry and Technology*, 79(3), pp.429–459.

Saavedra Flores, E.I., De Souza Neto, E. A. & Pearce, C., 2011. A large strain computational multi-scale model for the dissipative behaviour of wood cell-wall. *Computational Materials Science*, 50(3), pp.1202–1211.

Salmén, L., 2004. Micromechanical understanding of the cell-wall structure. *Comptes Rendus Biologies*, 327(9-10), pp.873–880.

Salmén, L., 1982. *Temperature and water induced softening behaviour of wood fiber based materials*, Phd Thesis, Royal Institute of Technology, Stockholm, Sweden.

Tanahashi, M., 1990. Characterization and Degradation Mechanisms of Wood Components by Steam Explosion and Utilization of Exploded Wood. *Wood Research*, 77, pp.49–117.

Thuvander, F., Kifetew, G. & Berglund, L.A., 2002. Modeling of cell wall drying stresses in wood. *Wood Science and Technology*, 36(3), pp.241–254.

Uhmeier, A. & Salmén, L., 1996. Influence of Strain Rate and Temperature on the Radial Compression Behavior of Wet Spruce. *Journal of Engineering Materials and Technology*, 118(3), pp.289–294.